PHYTOCHROMES B1/B2 ARE KEY REGULATORS OF EPIGENOME REPROGRAMMING DURING TOMATO FRUIT DEVELOPMENT

Ricardo Bianchetti[1], Nicolas Bellora[2], Luis A de Haro[3], Rafael Zuccarelli[1], Daniele Rosado[1§], Luciano Freschi[1], Magdalena Rossi[1,6], Luisa Bermudez[4,5*]

[1]Departamento de Botânica, Instituto de Biociências, Universidade de São Paulo, São Paulo, Brasil.

[2]Instituto Andino Patagónico de Tecnologias Biológicas y Geoambientales - CCT-CONICET, Patagonia Norte, Bariloche, Argentina.

[3]Department of Plant and Environmental Sciences, Weizmann Institute of Science, Rehovot, Israel.

[4]Instituto de Agrobiotecnología y Biología Molecular (IABIMO), CICVyA, INTA-CONICET, Argentina.

[5]Cátedra de Genética, Facultad de Agronomía, Universidad de Buenos Aires, Buenos Aires, Argentina.

[6] Senior author.

[§]Current address: Cold Spring Harbor Laboratory, Cold Spring Harbor, New York, USA.

* Corresponding Author.

Luisa Bermúdez

Phone: +54 11 4621 1447

email: bermudez.luisa@inta.gob.ar

Short Title: **PHYB1/B2 DEFFICIENCY ALTERS THE TOMATO FRUIT EPIGENOME**

Abstract

Phytochrome-mediated light and temperature perception has been shown to be a major regulator of fruit development. Furthermore, chromatin remodelling via DNA demethylation has been described as a crucial mechanism behind the fruit ripening process; however, the molecular basis underlying the triggering of this epigenetic modification remains largely unknown. Here, an integrative analyses of the methylome, siRNAome and transcriptome of tomato fruits from *phyA* and *phyB1B2* null mutants was performed, revealing that PHYB1 and PHYB2 influences genome-wide DNA methylation during fruit development and ripening. The experimental evidence indicates that PHYB1B2 signal transduction relies on a gene expression network that includes chromatin organization factors (DNA methylases/demethylases, histone-modifying enzymes and remodelling factors) and transcriptional regulators, ultimately leading to altered mRNA profile of photosynthetic and ripening-associated genes. This new level of understanding provides insights into the orchestration of epigenetic mechanisms in response to environmental cues affecting agronomical traits in fleshy fruits.

Keywords: carotenoid, chlorophyll, DNA methylation, epigenetics, fleshy fruit, phytochrome, RNA-seq, RdDM, tomato.

INTRODUCTION

As sessile organisms, plants must constantly monitor their environment and continuously tune their gene expression to enable adaptation and survival (Kaiserli et al., 2018). Light is one of the main environmental cues that controls plant growth and development from seed germination to senescence (Galvão and Fankhauser, 2015). Plants employ different photoreceptors to detect and respond to changes in the incident spectral composition (from UV-B to far-red wavelengths), light direction and photoperiod. These photoreceptor families include (i) phytochromes (PHYs), which perceive red/far-red (R/FR) light; (ii) cryptochromes (CRYs), phototropins, and 'Zeitlupes', which sense blue/UV-A light; and (iii) the UV-B receptor UVR8 (Paik and Huq, 2019).

After photoreceptor activation, complex signal transduction pathways control the expression of light-regulated genes via transcriptional, posttranscriptional, and posttranslational mechanisms (Galvão and Fankhauser, 2015). Several hub proteins in the light signal transduction pathway triggered by PHYs, CRYs and UVR8 have been identified, including transcription factors (TFs) such as PHY-INTERACTING FACTORS (PIFs) and ELONGATED HYPOCOTYL5 (HY5) as well as the ubiquitin E3 ligase complex comprising CONSTITUTIVE PHOTOMORPHOGENIC1 (COP1) (Galvão and Fankhauser, 2015). Moreover, both PHYA and PHYB can directly bind to target promoters (Chen et al., 2014; Jung et al., 2016), and the effect of light on alternative splicing (AS) has recently been described (Cheng and Tu, 2018). In *Arabidopsis thaliana*, 1,505 genes undergo changes in the AS levels of their transcripts within 1 h of exposure to red light in a PHY-dependent manner (Shikata et al., 2014). Similarly, in the moss *Physcomitrella patens*, 8.4% and 8.9% of AS events rapidly respond to PHY-mediated red and blue light perception (Wu et al., 2014). Further studies showed that the interaction between PpPHY4 and a splicing factor coregulates 70% of intron retention (IR) events in response to red light in *P. patens* (Lin et al., 2020). Moreover, light controls protein localization through PHY-mediated alternative promoter selection, allowing plants to metabolically respond to changing light conditions (Ushijima et al., 2017). Finally, it is widely known that activated PHYs induce post-translational changes in PIF proteins, including sequestration, phosphorylation, polyubiquitylation, and subsequent degradation through the 26S proteasome-mediated

pathway (Paik and Huq, 2019). Although the effect of light on plant phenotypes and the plant transcriptome has been studied for decades (Mazzella et al., 2005; Ibarra et al., 2013; Carlson et al., 2019), the involvement of epigenetic regulatory mechanisms in light-dependent changes in the transcriptional landscape remains poorly addressed.

Posttranslational histone modifications, such as acetylation and methylation, have been associated with the induction and repression of light-responsive genes (Perrella and Kaiserli, 2016; Tessadori et al., 2009). Light-dependent enrichment of the acetylation pattern of H3 and H4 in the enhancer and promoter regions of the pea plastocyanin locus *PetE* has been reported (Chua et al., 2001), and the hyperacetylation of the *PetE* promoter is linked to the transcriptional activity of this gene (Chua et al., 2003). Moreover, a reduction in H3 acetylation is associated with a decrease in the expression of the *A. thaliana* light-responsive genes CHLOROPHYLL a/b-BINDING PROTEIN GENE (CAB2) and the RIBULOSE BISPHOSPHATE CARBOXYLASE/OXYGENASE small subunit (RBCS) (Bertrand et al., 2005). Histone methylation regulates PHY-mediated seed germination in *A. thaliana*. Upon R light illumination, photoactivated PHYB (Pfr) targets PIF1 for proteasome-mediated degradation, releasing the expression of the JUMONJI HISTONE DEMETHYLASES JMJ20 and JMJ22. As a result, JMJ20 and JMJ22 reduce the levels of H4R3me2, which leads to the activation of the gibberellic acid biosynthesis pathway to promote seed germination (Cho et al., 2012).

Together with histone modification, DNA methylation is a common epigenetic mark with a direct impact on gene expression. Nevertheless, only a few reports have specifically addressed the effect of light stimuli on DNA methylation. Light-dependent nuclear organization dynamics during deetiolation are associated with a reduction in methylated DNA (Bourbousse et al., 2020). In *Populus nigra*, 137 genes were shown to be regulated by methylation during the day/night cycle (Ding et al., 2018). Moreover, photoperiod-sensitive male sterility is regulated by RNA-directed DNA methylation (RdDM) in rice (Ding et al., 2012). Finally, using a methylation-sensitive amplified polymorphism assay, DNA methylation remodelling was shown to be an active epigenetic response to different light qualities in tomato seedlings (Omidvar and Fellner, 2015).

Previous studies have shown that PHYA, PHYB1 and PHYB2 are major regulators of *Solanum lycopersicum* fruit ripening and nutraceutical compounds accumulation (Gupta et

al., 2014; Llorente et al., 2016; Alves et al., 2020; Gramegna et al., 2019; Bianchetti et al., 2018; Bianchetti et al., 2020). Moreover, it has also been shown that tomato fruit ripening involves epigenome reprogramming (Zhong et al., 2013). Here, genome-wide transcriptome, siRNAome and methylome were comprehensively analysed in fruits from *phyA* and *phyB1B2* null mutants, revealing that PHY signalling transduction modulates DNA methylation status from green towards ripe stages that, in turn, is a crucial gene expression regulatory mechanism along fruit development.

RESULTS

Impact of light perception impairment on the fruit transcriptome

To investigate the role played by either PHYA or PHYB1/PHYB2 (hereafter PHYB1B2) in overall gene expression during fruit development, the transcriptome of fruits at the immature green (IG) and breaker (BK) stages from *phyA* and *phyB1B2* null mutants as well as their wild-type (WT) counterpart, was determined by RNAseq. Among the approximately 20,000 transcriptionally active loci in each biological replicate (Supplemental Table 1), 1.2% and 2.4% at the IG stage and 9.1% and 11.2% at the BK stage were identified as differentially expressed genes (DEGs) in *phyA* or *phyB1B2* mutants, respectively, compared to the WT (Figure 1A; Supplemental Table 2). For both genotypes, the number of exclusive DEGs was significantly lower in the IG stage than in the BK stage; similarly, the number of genes that were commonly regulated by PHYA and PHYB1B2 was 172 at the IG stage and 785 at the BK stage (Figure 1B). Subsequently, the altered expression of approximately 76% (23/30) of the tested genes was validated by RT-qPCR (Supplemental Table 3). Comparison with previously reported expression data for genes involved in ripening regulation, ethylene biosynthesis and signalling, and carotenogenesis further validated our RNAseq data, as 90% of the analysed genes on average showed the expected mRNA profile at IG and BK stages. It is worth mentioning that most of the genes displayed the same transcript fluctuation in the WT, *phyA* and *phyB1B2* genotypes, though this was somewhat attenuated in the mutants (Supplemental Table 4). These results showed that PHY-meditated light perception regulates

more genes in BK than in the early stages of fruit development and that PHYB1B2 has a more substantial impact than PHYA in the fruit transcriptome in both analysed stages.

A closer look at DEGs function revealed a similar distribution of loci across MapMan categories in response to *phyB1B2* and *phyA* mutations in both developmental stages, although with distinct abundance levels (Figure 1C). At the IG stage, eight categories were mainly represented, including at least 2% of the DEGs identified in *phyA* and *phyB1B2*: photosynthesis, lipid metabolism, phytohormone action, RNA biosynthesis, protein modification, protein homeostasis, cell wall organization, and solute transport (Figure 1C; Supplemental Tables 5 and 6). It is worth highlighting the abundance of the DEGs within the photosynthesis category in the *phyB1B2* mutant, among which 34 out of the 37 genes were downregulated (Supplemental Table 6). In the BK stage, at least 2% of the DEGs were related to the lipid metabolism, phytohormone action, RNA biosynthesis, protein modification and homeostasis, cell wall organization and solute transport categories in both genotypes (Figure 1C; Supplemental Tables 7 and 8). However, while *phyA* deficiency also affected carbohydrate metabolism and external stimuli (Supplemental Table 7), the *phyB1B2* mutant showed a large number of DEGs related to the cell cycle and chromatin organization (Supplemental Table 8). Interestingly, the chromatin organization category displayed 52 DEGs, 45 of which were upregulated. These genes encode nucleosome constituent histones (H3, H4, H2A and H2B); DNA methylases/demethylases; histone post-translational modifiers such as deacetylases, methylases/demethylases, histone ubiquitination factors and histone chaperones; chromatin remodelling factors; and genes involved in RNA-independent and RNA-directed DNA methylation (Supplemental Table 8). These results led us to further investigate the impact of DNA methylation on PHY-mediated gene expression reprogramming.

PHYs-dependent reprogramming of tomato fruit methylome

The global profile of methylated cytosines (mCs) in the epigenome of tomato fruits was assessed by whole-genome bisulfite sequencing in the IG and BK stages for *phyA*, *phyB1B2* and WT genotypes. In agreement with previous reports (Zhong et al., 2013; Zuo et al., 2020), regardless of the genotype and fruit stage, the greatest total number of mCs was located in the CHH context, followed by the CG and CHG contexts, while the methylation level was

highest in the CG (80%) context followed by the CHG (67%) and CHH (23%) contexts (Supplemental Table 9, Supplemental Figure 1). For further comparisons, we selected only cytosines with coverage >10X, and except for chromosome 9 in the transposable elements TEs enriched region, all samples met this cutoff. In all contexts, the highest cytosine density was associated with gene-rich euchromatic regions located at chromosome arm ends (Supplemental Figure 1). Conversely, in symmetrical contexts (CG and CHG), the highest methylation rates were found across pericentromeric regions enriched in TEs, while the highest methylation rates in CHH context was observed in gene-rich regions associated with a higher density of sRNAs (Supplemental Figure 1). The comparison of the methylation status between the two fruit stages showed that ripening-associated demethylation (Zhong et al., 2013) occurs mainly in the CG context, especially in gene-rich regions, and that it is impaired in *phyB1B2* mutant BK fruits (Supplemental Figure 1).

The subsequent comparison between genotypes revealed global epigenome alteration in *phy* mutants in all contexts analysed. The most remarkable observation was the presence of considerable hypermethylation in all contexts across gene-rich regions in BK-stage fruits from *phyB1B2* (Figure 2A). In contrast, *phyA* exhibited hypermethylation in CHG and CHH contexts associated with TE-rich regions (Figure 2A), suggesting that different PHYs control DNA methylation across specific genomic regions through distinct regulatory mechanisms. Interestingly, PHY-associated hypomethylation was exclusively detected in the CG context of gene-rich regions in IG-stage fruits from *phyA* and in the CHH context of TE-rich regions for BK-stage fruits from *phyB1B2*. In summary, these data revealed that both PHYA and PHYB1B2 affect the global methylome, but PHYB1B2 has a greater impact on ripening-associated methylation reprogramming across gene-rich genomic regions in tomato fruits.

To investigate the relationship between PHY-dependent modifications in cytosine methylation and gene expression, we first identified genes with differentially methylated promoters (DMPs, 2 kb upstream of the transcription start site) in all three contexts. Interestingly, associated with the massive alteration previously observed, the pattern of DMPs varied with the mC context, stage and genotype (Figure 2B, Supplemental Table 10 and 11). Regarding the CG context, whereas the *phyA* mutant showed virtually the same frequency of hyper- and hypomethylated promoters in the two stages, the status of hypermethylated promoters in *phyB1B2* increased over 60% from the IG to BK stage, while

the number of loci with hypomethylation decreased 50% (Figure 2B, Supplemental Table 12). In contrast, *phyA* showed a greater number of hypermethylated promoters in the CHG context in the IG stage than in the BK stage, while the levels in the WT and *phyB1B2* mutant remained similar upon ripening (Figure 2B, Supplemental Table 13). In the CHH context, the number of hypermethylated promoters decreased in both genotypes from the IG to BK stages (Figure 2B, Supplemental Table 14).

These results indicate that PHY deficiency results in massive promoter hypermethylation in both the IG and BK stages of tomato fruit development. Moreover, they reinforce the role of PHYB1B2 in ripening-associated demethylation and its putative effect on gene expression.

Effect of PHY-mediated differential methylation on the transcriptome

To assess whether the differential methylation of gene promoters affects mRNA levels, we crossed data from DEGs and DMPs between genotypes. Supplemental Figure 2 shows scatter plots of promoter methylation vs mRNA fold changes for comparisons of the two genotypes at the two examined developmental stages in the three mC contexts. The most evident result was that among the thousands of loci with identified DMPs (Figure 2B), only hundreds of the loci were also differentially expressed (Supplemental Table 15) (0.7% for IG *phyA*, 1.6% for IG *phyB1B2*, 5.6% for BK *phyA* and 7.4% for BK *phyB1B2*), raising an intriguing question about the biological significance of the extensive change in the methylation pattern observed in the mutants. In contrast, the percentages of the DEGs showing DMPs were 73% for IG *phyA*, 76% for IG *phyB1B2*, 72% for BK *phyA* and 75% for BK *phyB1B2* (Supplemental Figure 2). Many more DEGs with DMPs were observed in BK than in IG fruits and in *phyB1B2* than in the *phyA* genotype. The functional categorization of these genes revealed a similar category distribution to the DEGs (Figure 1C, Supplemental Tables 16-19). At the IG stage, there were seven categories in which at least 2% of the loci showed DMPs and differential expression in both genotypes: photosynthesis, phytohormone action, RNA biosynthesis, protein modification and homeostasis, cell wall organization and solute transport, whereas *phyB1B2* additionally impacted lipid metabolism (Figure 1C). In the BK stage, the categories in which at least 2% of the DEGs showed DMPs were lipid metabolism, phytohormone action, RNA biosynthesis, protein modification and homeostasis, cell wall organization and solute transport-related functions in both genotypes, while only *phyA*

impacted carbohydrate metabolism and external stimuli, and only *phyB1B2* affected photosynthesis, chromatin organization and cell cycle categories.

Interestingly, in the comparison of the IG and BK stages, 42.5%, 34.2% and 18.8% of the DMPs were associated with DEGs, while 79.5%, 76.6% and 71.5% of the DEGs showed differences in promoter methylation in WT, *phyA* and *phyB1B2*, respectively (Supplemental Figure 3). All of these data demonstrated that the altered mRNA profile oh *phyA* and *phyB1B2* fruits are associated with marked changes in promoter methylation; however, massive genome-wide PHY-induced methylation reprogramming has a still uncharacterized role beyond the regulation of mRNA accumulation. Moreover, promoter methylation has a greater effect on gene expression regulation during BK than in the IG stage. Additionally, the data showed that PHYB1B2 has a more extensive influence on gene expression regulated via promoter methylation than PHYA, reinforcing the above conclusion that PHYB1B2 affects CG ripening-associated demethylation (Supplemental Figure 2).

The sRNAome is altered by PHY deficiency

To assess the involvement of RdDM in PHY-mediated transcriptome regulation, the sRNAome was analysed in fruits at the IG and BK stages from both mutants and the WT genotype (Supplemental Table 20A). A total of 28,314 clusters of sRNAs were identified across the whole genome in at least one of the samples, including 7,984 in gene bodies, 7,863 in promoter regions, 7,966 in TEs and the remaining 4,501 across intergenic regions (Supplemental Figure 1, Supplemental Table 20B). The methylation level was evaluated for each sRNA cluster-targeted genomic region (sCTGR), and as previously observed for promoter regions, a higher proportion of hypermethylation was observed in BK fruits from *phyB1B2* in the CG symmetrical context. Moreover, the greatest number of differentially methylated sCTGRs was observed in the asymmetrical context CHH (Figure 3A, Supplemental Table 20G-J).

sCTGR methylation levels and sRNA accumulation data were intersected, and among a total of 154, 318, 267 and 257 differentially accumulated sRNA clusters (Supplemental Table 20C-F), 88, 154, 99 and 82 also showed differential methylation changes (>5%) in *phyA* IG, *phyB1B2* IG, *phyA* BK and *phyB1B2* BK fruits, respectively (Figure 3B, (Supplemental Table 20G-J), showing a strong association ($P<0.005$) of the two datasets. Intriguingly, this positive

association was not observed in the transition from the IG to BK stages (Supplemental Figure 4), suggesting that the global methylation changes via RdDM could be attributed to PHY deficiency. Moreover, a clear disturbance in sRNA accumulation was observed in *phyB1B2*, since almost no clusters with less sRNA accumulation were observed in BK compared to the IG stage (Supplemental Figure 4). We further analysed whether this positive correlation observed between sRNA accumulation and sCTGR methylation impacted gene expression levels. Notably, regardless of the fruit developmental stage, changes in the accumulation of sRNA located in gene bodies (GBs), and not in the promoter (P) region, were positively correlated with the mRNA level (Figure 3C, Supplemental Table 20K-N). Among these loci, two interesting examples were identified: the well-known ripening-associated genes *RIPENING INHIBITOR* (*RIN*, Solyc05g012020 (Vrebalov et al., 2002)) and *FRUITFULL2* (*FUL2*, Solyc03g114830 (Bemer et al., 2012)), which showed higher expression in *phyB1B2* at the IG stage (Figure 4A) and higher sRNA accumulation and sCTGR methylation across their GBs (Figure 4B) compared to WT. The premature expression of these TFs was in agreement with the previously reported anticipation of ripening onset in the *phyB1B2* mutant (Gupta et al., 2014). Altogether, these findings revealed (i) impaired RdDM in BK fruits of *phyB1B2*, indicated by the absence of clusters with less sRNA accumulation, and (ii) that GB RdDM is an important mechanism that positively regulates gene expression in a PHY-mediated manner during fruit development.

PHYB1B2-dependent methylation regulates fruit chlorophyll accumulation

The categorization of DEGs associated with differential promoter methylation revealed prominent representation of the photosynthesis category in the fruits of the *phyB1B2* mutant at the IG stage (Figure 1C). Among the 32 genes, 22 were downregulated and hypermethylated in the promoter region (Supplemental Tables 6 and 17). Most of these genes encode chlorophyll-binding proteins, structural photosystem proteins and chlorophyll biosynthetic enzymes. This might at least partly explain the reduction of 50% in the total chlorophyll level observed in *phyB1B2* IG fruits (Figure 5A). Detailed promoter analysis of the chlorophyll-related enzymes *PROTOCHLOROPHYLLIDE OXIDOREDUCTASE 3* (*POR3*, Solyc07g054210), and two CHLOROPHYLL A/B BINDING PROTEINs (*CBP*, Solyc02g070990 and *CAB-3c*, Solyc03g005780) showed that the reduced mRNA levels of

these three genes in *phyB1B2* (Figure 5B) were correlated with the presence of hypermethylated regions in the promoters. Interestingly, several of these hypermethylated sequences overlapped with HY5 and PIF photomorphogenic TF binding sites, such as G-box (CACGTG), CA hybrid (GACGTA), CG hybrid (GACGTG) and PBE-box (CACATG) motifs (Zhang et al., 2013) (Figure 5C). These results suggest that the transcription of genes involved in chlorophyll metabolism and the photosynthetic machinery in tomato fruits is regulated by the PHYB1B2-dependent methylation status of their promoter regions in addition to the PHY-mediated post-translational regulation of HY5 and PIF protein levels (Galvão and Fankhauser, 2015).

The methylation-mediated regulation of fruit ripening is influenced by PHYB1B2 signalling

In their seminal study, Zhong et al. (2013) revealed that the extensive methylation in the promoter regions of ripening-associated genes gradually decreases during fruit development. Interestingly, RNA biosynthesis, which includes transcription factors, was the most abundant functional category among the DEGs that showed DMPs (Figure 1C). Thus, we examined a set of ripening-associated transcription factors: *RIN*, Solyc05g012020, *NON-RIPENING* (*NOR*, Solyc10g006880 (Giovannoni, 2007)), *COLORLESS NORIPENING* (*CNR*, Solyc02g077920 (Manning et al., 2006)) and *APETALA2a* (*AP2a*, Solyc03g044300 (Karlova et al., 2011)). The evaluation of the promoter regions clearly showed that while their methylation level decreased from the IG to BK stage in the WT genotype, they remained highly methylated in *phyB1B2* (Figure 6A). As previously observed, several hypermethylated regions are closely linked to HY5 and PIF binding sites. The maintenance of high methylation levels in the promoters of these key regulatory genes at the onset of fruit ripening was highly correlated with their transcriptional downregulation at the BK stage (Figure 6B).

Carotenoid accumulation is probably the most appealing and best investigated trait of tomato fruits; in agreement with previous findings (Bianchetti et al., 2020), ripe *phyB1B2* fruits showed a five-fold reduction in carotenoid content compared to WT (Figure 7A).

With the aim of evaluating whether this effect is a consequence of the methylation-mediated regulation of carotenoid biosynthesis genes, we further analysed the promoters of *PHYTOENE SYNTHASE 1* (*PSY1*, Solyc03g031860), *PHYTOENE DESATURASE* (*PDS*,

Solyc03g123760), *15-CIS- ζ-CAROTENE* (*ZISO*, Solyc12g098710) and *ZETA-CAROTENE DESATURASE* (*ZDS*, Solyc01g097810), which, with the exception of *PDS*, were hypermethylated in *phyB1B2* BK fruits (Supplemental Table 11). The mC profile confirmed the presence of hypermethylated regions in all four promoters, which were predominantly located near light-dependent TF binding motifs in the *PSY1*, *PDS* and *ZISO* promoters (Figure 7B), explaining the reduced mRNA levels of these genes observed in *phyB1B2* (Figure 7C).

RIN is one of the main TFs controlling ripening-associated genes by directly binding to their promoters. RIN binding occurs in concert with the demethylation of its targets (Zhong et al., 2013). To examine whether RIN binding site methylation could be affected by the *phyB1B2* mutation in the ripening-related master transcription factors and carotenoid biosynthesis gene promoters, we mapped the available RIN ChIP-seq data (Zhong et al., 2013) and performed *de novo* motif discovery (Supplemental Figure 5). Interestingly, the levels of mCs associated with RIN targets were higher in the *NOR*, *CNR* and *AP2a* promoters in *phyB1B2* than in WT. Moreover, the *RIN* promoter itself was hypermethylated across the RIN binding site in *phyB1B2* BK fruits, suggesting a positive feedback regulatory mechanism (Figure 6A). Finally, in the *phyB1B2* mutant, the *PSY1*, *PDS*, *ZISO* and *ZDS* promoters showed higher methylation overlapping with RIN target binding sites, indicating that the upregulation of carotenoid biosynthesis genes during tomato ripening is dependent on the PHYB1B2-mediated demethylation of RIN target sites.

Altogether, our findings showed that PHYB1B2 is a major player in fruit ripening by affecting the promoter demethylation of master transcriptional regulators and carotenoid biosynthesis genes.

DISCUSSION

The dynamic methylation pattern during tomato fruit development has been demonstrated to be a critical ripening regulation mechanism (Zhong et al., 2013; Zuo et al., 2020). DNA demethylation, mainly in the CG context, triggers the activation of genes involved in ripening and is required for pigment accumulation and ethylene synthesis (Zhong et al., 2013; Lang et al., 2017). Simultaneously, the dynamic epigenome during fruit development is strictly regulated by environmental cues (Zhang et al., 2016). The prevailing model establishes PHYs

as major components involved in the coordination of fruit physiology with the ever-changing light and temperature environment (Alves et al., 2020; Bianchetti et al., 2020). Thus, we explored the link between fruit epigenome reprogramming and these well-established light and temperature sensors (Legris et al., 2016).

Our data clearly showed that *phyA* and *phyB1B2* deficiencies modified the epigenome profile through methylome and sRNAome reprogramming. In particular, PHY-mediated DMPs and GB methylation impacted the transcriptome pattern, affecting tomato fruit development and demonstrating that a portion of the ripening-associated demethylation previously reported (Zhong et al., 2013) is dependent on active PHYs, especially PHYB1B2. However, the massive alteration of methylation patterns observed in *phy* mutants suggests the existence of a still unclear genome regulatory mechanism. Whether it is related to light-induced AS (Cheng and Tu, 2018) and/or PHY-mediated alternative promoter usage to control protein localization (Ushijima et al., 2017), as mentioned above, remains to be explored.

The *phyA* and *phyB1B2* mutants showed a positive correlation between cluster sRNA accumulation, target methylation in GB and mRNA levels. In angiosperms, GB methylation has been associated with constitutively expressed genes (Bewick and Schmitz, 2017; Lu et al., 2015); however, PHY deficiency intriguingly seems to deregulate this mechanism, affecting the temporally expression of regulated genes. The *RIN* and *FUL2* examples analysed here clearly showed that sRNA accumulation and methylation were mainly located near transposable elements (TEs) (Figure 4). It is known that the insertion of TEs within GB can disrupt gene expression; thus, methylation-mediated TE silencing and GB methylation are evolutionarily linked (Bewick and Schmitz, 2017). The enhancement of TE-associated DNA methylation in GB (Figure 3C) and the absence of clusters with less sRNA accumulation in BK compared to the IG stage in *phyB1B2* (Supplemental Figure 4) can be explained by the overexpression of canonical RdDM genes. Solyc12g008420 and Solyc06g050510 encode homologs of RNA-DEPENDENT RNA POLYMERASE (RDRP) and the associated factor SNF2 DOMAIN-CONTAINING PROTEIN CLASSY 1 (CLSY1), respectively, both of which were upregulated in BK fruits from *phyB1B2* plants (Supplemental Table 2). These proteins are key players in canonical RdDM in *A. thaliana* required for PolIV-dependent sRNA production (Zhang et al., 2018). Similarly, Solyc09g082480 and Solyc03g083170, which were also upregulated in *phyB1B2* BK fruits,

are homologs of *A. thaliana* RNA-DIRECTED DNA METHYLATION 1 (RDM1) and DEFECTIVE IN MERISTEM SILENCING 3 (DMS3), respectively. The protein products of these genes, together with DEFECTIVE IN RNA- DIRECTED DNA METHYLATION 1 (DRD1), form the DDR complex, which enables RNA Pol V transcription (Pikaard and Scheid, 2014). To our knowledge, this is the first report to associate PHY-mediated sRNA accumulation and DNA methylation with mRNA levels in plants.

Several pieces of evidence have shown that PHYB1B2 has a more substantial impact on tomato genome regulation than PHYA. For example, BK fruits from *phyB1B2* displayed (i) a large number of DEGs associated with chromatin organization (Figure 1C); (ii) overall promoter hypermethylation in the CG context (Figure 2B); (iii) the highest number of DEGs associated with DMPs (Supplemental Figure 2); and (iv) half the number of DMPs associated with DEGs between the IG and BK stages compared to the WT (Supplemental Figure 3). These massive epigenomic alterations in *phyB1B2* led us to look more closely at genes related to chromatin organization that showed alterations in mRNA levels.

The chromomethylase *SlMET1L* (Solyc01g006100) (also referred to as *SlCMT3* (Gallusci et al., 2016)) displays the highest transcript abundance in immature fruits, which declines towards the fully ripe stage (Cao et al., 2014). Hence, in line with the higher level of DNA methylation, our transcriptome analysis showed that *SlMET1L* was upregulated in *phyB1B2* BK fruits. Conversely, the upregulation of the *SlROS1L* demethylase (Solyc09g009080 (Cao et al., 2014), also referred to as *SlDML1* (Liu et al., 2015), was also observed in *phyB1B2* BK fruits, which might seem contradictory at first glance. However, it has been reported that the *Arabidopsis thaliana ROS1* gene promoter contains a DNA methylation monitoring sequence (MEMS) associated with a Helitron transposon, which is methylated by AtMET1, positively regulating *AtROS1* gene expression (Lei et al., 2015). Similarly, *SlROS1L* harbours two transposable elements within its promoter and showed a higher methylation level in *phyB1B2* than in the WT genotype, suggesting a similar regulatory mechanism in tomato (Supplemental Figure 6, Supplemental Table 15).

The tomato homologue of *A. thaliana* DECREASED DNA METHYLATION 1 (DDM1, Solyc02g085390) showed higher mRNA expression in *phyB1B2* mutant BK fruits than in their WT counterparts. DDM1 is a chromatin remodelling protein required for maintaining DNA methylation in the symmetric cytosine sequence (Zemach et al., 2013), which can be

associated with the observed methylation differences in the CG context in *phyB1B2* (Figure 2A).

Several histone modifiers showed altered expression in BK fruits from the *phyB1B2* mutant (Supplemental Table 8). The methylation of lysine residues 9 and 27 on histone H3 is associated with repressed genes. Histone lysine methyltransferases are classified into five groups based on their domain architecture and/or differences in enzymatic activity (Pontvianne et al., 2010). The BK fruits of the *phyB1B2* mutant displayed three differentially expressed lysine methyltransferases: Solyc03g082860, an upregulated H3K27 Class IV homologue, and Solyc06g008130 and Solyc06g083760, two H3K9 Class V homologs that showed lower and higher expression than in WT fruits, respectively. Histone arginine methylation is catalysed by a family of enzymes known as protein arginine methyltransferases (PRMTs). Solyc12g099560, a PRMT4a/b homologue, was upregulated in *phyB1B2* BK fruits. Interestingly, in *A. thaliana*, PRMT4s modulate key regulatory genes associated with the light response (Hernando et al., 2015), reinforcing the link between the PHYB1B2 photoreceptor and epigenetic control. Finally, tomato histone demethylases have been recently identified. *SlJMJ6*, whose expression peaks immediately after the BK stage, has been characterized as a positive regulator of fruit ripening by removing the H3K27 methylation of ripening-related genes, and *SlJMJ6*-overexpressing lines show increased carotenoid levels (Li et al., 2020). *SlJMJC1* (Solyc01g006680), which exhibits the same expression pattern (Li et al., 2020), is downregulated in the *phyB1B2* mutant, suggesting that this gene might exhibit a similar regulatory function to its paralogue, inducing ripening in a PHYB1B2-dependent manner (Figures 6 and 7).

Histone deacetylation plays a crucial role in the regulation of eukaryotic gene activity and is associated with inactive chromatin (Zhang et al., 2018). Histone deacetylation is catalysed by histone deacetylases (HDACs). Fifteen HDACs were identified in the tomato genome (Zhao et al., 2015). Among these HDACs, *SlHDA10* (Solyc01g009120) and *SlHDT3* (Solyc11g066840) were found to be downregulated and upregulated in *phyB1B2* BK fruits, respectively. SlHDA10 is localized in the chloroplast, and its transcript is highly expressed in photosynthetic tissues (Zhao et al., 2015); whether SlHDA10 deacetylates chloroplast proteins by silencing photosynthesis-related genes remains to be determined. Although *SlHDT3* is mainly expressed in immature stages of fruit development and its expression

declines with ripening, its silencing results in delayed ripening and reduced *RIN* expression and carotenogenesis. On the other hand, the expression level of *SlHDT3* is increased in ripening-deficient mutants such as *Nr* or *rin* (Guo et al., 2017). Our results showed that *phyB1B2* mutant fruits displayed higher expression of *SlHDT3* and reduced *RIN* transcript levels at the BK stage, suggesting reciprocal regulation between these two factors. Thus, we propose a model where during the IG stage, *SlHDT3* is highly expressed, contributing to the epigenetic inhibition of ripening. The reduction in *SlHDT3* expression towards BK releases DNA methylation that, in turn upregulates *RIN*. Additionally, PHYB1B2 inhibits the expression of *SlHDT3* and induces that of *RIN*, thereby inducing or repressing DNA methylation, respectively. Finally, RIN maintains *SlHDT3* downregulation in BK (Guo et al., 2017) (Figure 8A). This mechanism precisely tunes ripening-related epigenetic reprogramming and contributes to explaining the high methylation levels observed in the *phyB1B2* mutant (Figure 2).

The complex interactive module involving DNA methylation levels and tomato ripening-transcription factors has been previously reported (Zhong et al., 2013; Zuo et al., 2020), but the stimuli and the molecular mechanisms underlying this relationship remained unknown. The integrated analysis of the experimental evidence together with previous gene functional studies in tomato and *A. thaliana* allowed us to propose that PHYB1B2 is an important factor in this module triggering chromatin organization factors and transcriptional regulators leading to a shift in the expression profile along fruit development (Figure 8B). Whether PHYB1B2 itself and/or PHY-downstream transcription factors are these epigenome regulators remains to be unravelled (Chen et al., 2014; Jung et al., 2016). The vast reservoir of data released here brings a new level of understanding about how epigenetic mechanisms orchestrate the response to PHY-mediated light and temperature fluctuations affecting important agronomical traits in fleshy fruits.

MATERIAL AND METHODS

Plant material, growth conditions and sampling

phyA and *phyB1B2* phytochrome mutants in the *Solanum lycopersicum* (cv. MoneyMaker) genetic background were previously characterized (Kerckhoffs et al., 1996; Lazarova et al., 1998; Kerckhoffs et al., 1999). Plants were grown from April to July 2019, in a glasshouse at the Instituto de Biociências, Universidade de São Paulo, 23º33´55´´S 46º43´51´´W. Tomato seeds were grown in 9L pots containing a 1:1 mixture of commercial substrate and expanded vermiculite, supplemented with 1 g L^{-1} of NPK 10:10:10, 4 g L^{-1} of dolomite limestone ($MgCO_3$ + $CaCO_3$) and 2 g L^{-1} thermophosphate at 24/18 °C under a 16/8 h light/dark cycle under 230 - 250 µmol photons m^{-2} s^{-1} irradiation and a relative humidity of 55%. It has been reported the epigenome changes during tomato fruit development (Zhong et al., 2013). On the other hand, it is known that PHYs can affect ripening time, although WT, *phyA* and *phyB1B2* fruits reached the same size at the final of expansion phase (Gupta et al., 2014). Then, in order to avoid the noise of any eventual developmental alteration cause by the mutations, fruits were sampled at the same development stage instead of necessary the same age. Five replicates per genotype were cultivated, and fruits were sampled at the immature green (15 mm diameter), mature green (when the placenta displays a jelly aspect), breaker (beginning of ripening process when the fruit shows the first yellowish colouration) and red ripe (7 days after the breaker stage) stages. All fruits were harvested at the same time of day with four biological replicates (each replicate was composed of a single fruit per plant). The columella, placenta, and seeds were immediately removed, and the remaining tissues were frozen in liquid nitrogen, ground and freeze-dried for subsequent analysis.

Transcriptional profile

Total RNA was extracted from immature green and breaker stage fruits with three independent biological replicates of each genotype using a Promega ReliaPrep RNA tissue kit according to the manufacturer's instructions. The RNA concentration was determined with a spectrophotometer (Nanodrop ND-1000; NanoDrop Technologies, Wilmington, DE, U.S.A.), RNA quality was assessed with a BioAnalyzer 2100 (Agilent Technologies), and RNA libraries were constructed following the recommendations of an Illumina Kit (Directional mRNA-Seq Sample Preparation) and sequenced using the Illumina NovaSeq 6000 System. Each library was sequenced, generating approximately 20 million 150 bp paired end reads per sample. The raw sequencing reads that were generated were analysed

with FastQC (http://www.bioinformatics.babraham.ac.uk/projects/fastqc/) and were filtered and cleaned using Trimmomatic (Bolger et al., 2014) (Parameters: ILLUMINACLIP: TruSeq3-PE.fa:2:30:10LEADING:3 TRAILING:3 SLIDINGWINDOW:4:20 MINLEN:50). At least 95% (19.1-27.9 M) of the reads met the quality criteria and were mapped to the tomato reference genome sequence SL3.0 with the ITAG3.2 annotation using STAR v2.4.2. allowing one mismatch (Dobin et al., 2013), approximately 84% of the reads were uniquely mapped (Supplemental Table 1) and were used for statistical analysis.

Reverse transcription quantitative PCR (RT-qPCR)

Total RNA extraction was performed with the ReliaPrep™ RNA Cell and Tissue Miniprep System (Promega), and cDNA synthesis was conducted with SuperScript™ IV Reverse Transcriptase (Invitrogen). The primers used for qPCR are listed in Supplemental Table 21. RT-qPCR was performed in a QStudio6 – A1769 PCR Real-Time thermocycler using 2X Power SYBR Green Master Mix in a final volume of 10 µL. Absolute fluorescence data were analysed using LinRegPCR software to obtain Ct and primer efficiency values. Relative mRNA abundance was calculated and normalized according to the ΔΔCt method using *EXPRESSED* and *CAC* as reference genes (Expósito-Rodríguez et al., 2008).

MethylC-Seq analysis

Methyl C sequencing was performed as described in a previous report (Lister et al., 2008). gDNA (~5 g) was extracted from a pool of the same three biological replicates used in the transcriptome analyses, obtained from three IG and BK fruit samples per genotype, using the DNeasy Plant maxi kit (Qiagen). The libraries were prepared with the EZ DNA Methylation-Gold Kit (Zymo Research) and the Accel-NGS® Methyl-Seq DNA Library Kit (Swift Biosciences) and further sequenced using the Illumina NovaSeq 6000 platform. Over 240 M reads were sequenced from each genotype and stage. Raw reads were screened for quality using Trimmomatic (Bolger et al., 2014) (parameters: ILLUMINACLIP:TruSeq3-PE.fa:2:30:10 LEADING:3 TRAILING:3 SLIDINGWINDOW:4:20 MINLEN:50). Mapping to the tomato reference genome sequence SL3.0 and the assessment of global methylation status were performed using Bismark (Krueger and Andrews, 2011) (parameters: bismark -q --bowtie2 --non_directional -N 1 -p 4), and the methylation status of

DNA in the three possible contexts (CG, CHG and CHH) was distinguished. At least 130 M reads were uniquely mapped (Supplemental Table 9). The Bioconductor package methylKit (Akalin et al., 2012) was used for the detection of methylation levels across the analysed regions: promoters (2 kb upstream of transcription start site) and sRNA cluster-targeted genome regions (sCTGRs). Only Cs with 10X coverage were considered. Methylation differences with an FDR < 0.05 in each comparison (WT vs *phyA*; WT vs *phyB1B2*) were recorded as differentially methylated promoters (DMPs) or differentially methylated sCTGRs. Differential methylation in the CG, CHG and/or CHH context was considered to exist if the region contained at least 10 differentially methylated Cs in the corresponding context. Finally, for the comparison of global methylation levels between genotypes, only common Cs with at least 10X coverage in all samples were analysed.

sRNAome profile

sRNA extraction and quality parameters were determined from three independent biological replicates of green and breaker stage fruits from each genotype, as described above in the "Transcriptional profile" section. After RNA integrity confirmation, libraries were prepared using a TruSeq Small RNA Library Prep and sequenced using the Illumina HiSeq 4000 platform to generate a read length of 50 bp. The raw sequencing reads that were generated were quality trimmed with Trimmomatic (Bolger et al., 2014) to retain reads of 18-24 nt in length (parameters: ILLUMINACLIP:TruSeq3-SE:2:30:10 LEADING:3 TRAILING:3 SLIDINGWINDOW:4:15 MINLEN:18 AVGQUAL:25). A minimum of 38% (WT/breaker/A) and a maximum of 85% (WT/immature green/A) of the reads achieved the quality criteria and were used for further analyses (Supplemental Table 20A). All libraries were aligned to genome version SL3.0 using ShortStack v3.8.1 (Axtell, 2013) with default parameters (allowing the distribution of multimapping reads according to the local genomic context). Then, the *de novo* identification of clusters of sRNAs was performed for all libraries, and individual counts for each library and cluster were obtained using the same software.

Statistical analysis for RNAseq and sRNAome

Genes/sRNA clusters with read/count numbers smaller than two per million were removed. Read/count values were normalized according to the library size factors. Statistical analyses were performed with edgeR from Bioconductor® (Robinson et al., 2009; McCarthy et al., 2012) using a genewise negative binomial generalized linear model with the quasi-likelihood test (Chen et al., 2016) and a cutoff of the false discovery rate (FDR) ≤ 0.05.

Gene functional categorization

The DEGs were functionally categorized with MapMan application software (Thimm et al., 2004) followed by hand-curated annotation using MapMan categories.

***In silico* regulatory motif predictions and RIN ChIP-seq analyses**

To predict the transcription factor binding motifs, we used the complete collection of 530 plant transcription factor-binding sites (TFBS) modelled as position frequency matrices (PFMs) from the JASPAR 2020 database (Fornes et al., 2019). Putative binding sites were obtained by scanning the whole *S. lycopersicum* 3.00 genome with Fimo (Bailey et al., 2015), p-value < 1e−5.

RIN ChIPseq reads were downloaded from the Sequence Read Archive (SRA) (accession SRX15083 (Zhong et al., 2013) and mapped to tomato genome version SL3.0 with STAR (Dobin et al., 2013) (version 2.7.3X, parameters: outFilterMismatchNmax 3, alignEndsType EndToEnd, alignIntronMax 5), and peak calling was performed by using Macs2 (Zhang et al., 2008) (version 2.2.7.1, default parameters). Regions of 200 bp centred on the top-scoring peaks (score>100, n=327) among transposable elements were retrieved, and the binding motif was inferred *de novo* by using the MEME algorithm (Supplemental Figure 5) (Bailey et al., 2015).

Carotenoid and chlorophyll analysis

Carotenoid and chlorophyll extraction was performed from aliquots of 20 mg dry mass, sequentially with 100 µL of a saturated solution of NaCl, 200 µL of dichloromethane and 500 µL of hexane:diethyl ether 1:1 (v/v). The pellet was extracted three additional times with 500 µL of 1:1 (v/v) hexane:diethyl ether. All supernatant fractions were combined, completely dried by vacuum and suspended in 200 µL of acetonitrile. Chlorophyll, phytoene,

phytofluene, lycopene, β-carotene and lutein levels were determined via HPLC with a photodiode array detector (Lira et al., 2017).

Statistical analysis of RT-qPCR and metabolites

Statistical analyses of the RT-qPCR (Student's t-test, $p \leq 0{,}05$) and metabolic data (ANOVA, Tukey's test. $p \leq 0{,}05$) were performed with InfoStat/F software (http://www.infostat.com.ar).

ACKNOWLEDGMENTS

This work was supported by FAPESP (Fundação de Amparo à Pesquisa do Estado de São Paulo, Grant Number #2016/01128-9); RB was a recipient of a FAPESP fellowship (#2017/24354-7). MR was a recipient of a CNPq fellowship. LB was a recipient of a CAPES-PRINT scholarship (88887.370243/2019-00).

Author contributions

RB performed most of the experiments and analysed the data; LB, NB, LAH and RZ analysed the data; DR performed the experiments; RB, LF, MR and LB conceived the project, designed the experiments and wrote the paper, which was revised and approved by all authors. LB agrees to serve as the author responsible for contact and ensures communication.

Competing interests

The authors declare no competing interests.

Data availability

All high-throughput sequencing data reported in this paper have been uploaded to the Sequence Read Archive (SRA) under NCBI Bioproject PRJNA646733, with accession numbers SUB7763724, SUB7782168 and SUB7791358 for RNAseq, WGBS and small RNAseq, respectively.

References

Akalin, A., Kormaksson, M., Li, S., Garrett-Bakelman, F.E., Figueroa, M.E., Melnick,

A., and Mason, C.E. (2012). MethylKit: a comprehensive R package for the analysis of genome-wide DNA methylation profiles. Genome Biol. **13**: R87.

Alves, F.R.R., Lira, B.S., Pikart, F.C., Monteiro, S.S., Furlan, C.M., Purgatto, E., Pascoal, G.B., Andrade, S.C. da S., Demarco, D., Rossi, M., and Freschi, L. (2020). Beyond the limits of photoperception: constitutively active PHYTOCHROME B2 overexpression as a means of improving fruit nutritional quality in tomato. Plant Biotechnol. J. doi: 10.1111/pbi.13362.

Axtell, M.J. (2013). ShortStack: Comprehensive annotation and quantification of small RNA genes. Rna **19**: 740–751.

Bailey, T.L., Johnson, J., Grant, C.E., and Noble, W.S. (2015). The MEME Suite. Nucleic Acids Res. **43**: 39–49.

Bemer, M., Karlova, R., Ballester, A.R., Tikunov, Y.M., Bovy, A.G., Wolters-Arts, M., Rossetto, P. de B., Angenent, G.C., and de Maagd, R.A. (2012). The Tomato FRUITFULL Homologs TDR4/FUL1 and MBP7/FUL2 Regulate Ethylene-Independent Aspects of Fruit Ripening. Plant Cell **24**: 4437–4451.

Bertrand, C., Benhamed, M., Li, Y.-F., Ayadi, M., Lemonnier, G., Renou, J.-P., Delarue, M., and Zhou, D.-X. (2005). *Arabidopsis HAF2* gene encoding TATA-binding protein (TBP)-associated factor TAF1, is required to integrate light signals to regulate gene expression and growth. J. Biol. Chem. **280**: 1465–1473.

Bewick, A.J. and Schmitz, R.J. (2017). Gene body DNA methylation in plants. Curr. Opin. Plant Biol. **36**: 103–110.

B**ianchetti, R.E., Silvestre Lira, B., Santos Monteiro, S., Demarco, D., Purgatto, E., Rothan, C., Rossi, M., and Freschi, L.** (2018). Fruit-localized phytochromes regulate plastid biogenesis, starch synthesis, and carotenoid metabolism in tomato. J. Exp. Bot. **69**: 3573–3586.

Bianchetti, R. De Luca B., de Haro L.A., Rosado D., Demarco D., Conte M., Bermudez L., Freschi L., Fernie A.R., Michaelson L.V., Haslam R.P., Rossi M., and Carrari F. (2020). Phytochrome-Dependent Temperature Perception Modulates Isoprenoid Metabolism. Plant Physiol. **183**: 869–882.

Bolger, A.M., Lohse, M., and Usadel, B. (2014). Trimmomatic: A flexible trimmer for Illumina sequence data. Bioinformatics **30**: 2114–2120.

Bourbousse, C., Barneche, F., and Laloi, C. (2020). Plant Chromatin Catches the Sun. Front. Plant Sci. **10**: 1728.

Cao, D., Ju, Z., Gao, C., Mei, X., Fu, D., Zhu, H., Luo, Y., and Zhu, B. (2014). Genome-wide identification of cytosine-5 DNA methyltransferases and demethylases in *Solanum lycopersicum*. Gene **550**: 230–237.

Carlson, K.D., Bhogale, S., Anderson, D., Tomanek, L., and Madlung, A. (2019). Phytochrome a regulates carbon flux in dark grown tomato seedlings. Front. Plant Sci. **10**: 1–20.

Chen F., Li B., Li G., Charron J.B., Dai M., Shi X., and Deng X.W. (2014). *Arabidopsis* Phytochrome A Directly Targets Numerous Promoters for Individualized Modulation of Genes in a Wide Range of Pathways. Plant Cell **26**:1949-1966.

Chen, Y., Lun, A.T.L., and Smyth, G.K. (2016). From reads to genes to pathways: differential expression analysis of RNA-Seq experiments using Rsubread and the edgeR quasi-likelihood pipeline. F1000Research **5**: 1438.

Cheng, Y.-L. and Tu, S.-L. (2018). Alternative Splicing and Cross-Talk with Light Signaling. Plant Cell Physiol. **59**: 1104–1110.

Cho, J.-N., Ryu, J.-Y., Jeong, Y.-M., Park, J., Song, J.-J., Amasino, R.M., Noh, B., and Noh, Y.-S. (2012). Control of seed germination by light-induced histone arginine demethylation activity. Dev. Cell **22**: 736–748.

Chua, Y.L., Brown, A.P., and Gray, J.C. (2001). Targeted histone acetylation and altered nuclease accessibility over short regions of the pea plastocyanin gene. Plant Cell **13**: 599–612.

Chua, Y.L., Watson, L.A., and Gray, J.C. (2003). The transcriptional enhancer of the pea plastocyanin gene associates with the nuclear matrix and regulates gene expression through histone acetylation. Plant Cell **15**: 1468–1479.

Ding, C.J., Liang, L.X., Diao, S., Su, X.H., and Zhang, B.Y. (2018). Genome-wide analysis of day/night DNA methylation differences in *Populus nigra*. PLoS One **13**: 1–14.

Ding, J., Shen, J., Mao, H., Xie, W., Li, X., and Zhang, Q. (2012). RNA-directed DNA methylation is involved in regulating photoperiod-sensitive male sterility in rice. Mol. Plant **5**: 1210–1216.

Dobin, A., Davis, C.A., Schlesinger, F., Drenkow, J., Zaleski, C., Jha, S., Batut, P., Chaisson, M., and Gingeras, T.R. (2013). STAR: ultrafast universal RNA-seq aligner. Bioinformatics **29**: 15–21.

Expósito-Rodríguez, M., Borges, A.A., Borges-Pérez, A., and Pérez, J.A. (2008). Selection of internal control genes for quantitative real-time RT-PCR studies during tomato development process. BMC Plant Biol. **8**: 131.

Fornes, O.,Castro-Mondragon, J.A., Khan, A., van der Lee, R., Zhang, X., Richmond R.P., Modi, B.P., Correard, S., Gheorghe, M., Baranašić, D., Santana-Garcia, W., Tan, G., Chèneby, J., Ballester, B., Parcy, F., Sandelin, A., Lenhard, B., Wasserman, W.W., Mathelier, A. (2019). JASPAR 2020: update of the open-access database of transcription factor binding profiles. Nucleic Acids Res. **48**: 87–92.

Gallusci, P., Hodgman, C., Teyssier, E., and Seymour, G.B. (2016). DNA Methylation and Chromatin Regulation during Fleshy Fruit Development and Ripening . Front. Plant Sci. **7**: 807.

Galvão, V.C. and Fankhauser, C. (2015). Sensing the light environment in plants: photoreceptors and early signaling steps. Curr. Opin. Neurobiol. **34**: 46–53.

Giovannoni, J.J. (2007). Fruit ripening mutants yield insights into ripening control. Curr. Opin. Plant Biol. **10**: 283–289.

Gramegna, G., Rosado, D., Sánchez Carranza, A.P., Cruz, A.B., Simon-Moya, M., Llorente, B., Rodríguez-Concepcíon, M., Freschi, L., and Rossi, M. (2019). PHYTOCHROME-INTERACTING FACTOR 3 mediates light-dependent induction of tocopherol biosynthesis during tomato fruit ripening. Plant. Cell Environ. **42**: 1328–1339.

Guo, J.E., Hu, Z., Li, F., Zhang, L., Yu, X., Tang, B., and Chen, G. (2017). Silencing of histone deacetylase *SlHDT3* delays fruit ripening and suppresses carotenoid accumulation in tomato. Plant Sci. **265**: 29–38.

Gupta, S.K., Sharma, S., Santisree, P., Kilambi, H.V., Appenroth, K., Sreelakshmi, Y., Sharma, R. (2014). Complex and shifting interactions of phytochromes regulate fruit development in tomato. Plant. Cell Environ. **37**: 1688–1702.

Hernando, C.E., Sanchez, S.E., Mancini, E., and Yanovsky, M.J. (2015). Genome wide comparative analysis of the effects of PRMT5 and PRMT4/CARM1 arginine

methyltransferases on the *Arabidopsis thaliana* transcriptome. BMC Genomics **16**: 192.

Ibarra, S.E., Auge, G., Sánchez, R.A., and Botto, J.F. (2013). Transcriptional programs related to phytochrome a function in arabidopsis seed germination. Mol. Plant **6**: 1261–1273.

Jung J.H., Domijan M., Klose C., Biswas S., Ezer D., Gao M., Khattak A.K., Box M.S., Charoensawan V., Cortijo S., Kumar M., Grant A., Locke J.C., Schäfer E., Jaeger K.E., and Wigge P.A. (2016). Phytochromes function as thermosensors in *Arabidopsis*. Science **354**: 886–889.

Kaiserli, E., Perrella, G., and Davidson, M.L. (2018). Light and temperature shape nuclear architecture and gene expression. Curr. Opin. Plant Biol. **45**: 103–111.

Karlova, R., Rosin, F.M., Busscher-Lange, J., Parapunova, V., Do, P.T., Fernie, A.R., Fraser, P.D., Baxter, C., Angenent, G.C., and de Maagd, R.A. (2011). Transcriptome and Metabolite Profiling Show That APETALA2a Is a Major Regulator of Tomato Fruit Ripening. Plant Cell **23**: 923–941.

Kerckhoffs, L.H.J., Kelmenson, P.M., Schreuder, M.E.L., Kendrick, C.I., Kendrick, R.E., Hanhart, C.J., Koornneef, M., Pratt, L.H., and Cordonnier-Pratt, M.M. (1999). Characterization of the gene encoding the apoprotein of phytochrome B2 in tomato, and identification of molecular lesions in two mutant alleles. Mol. Gen. Genet. **261**: 901–907.

Kerckhoffs, L.H.J., Van Tuinen, A., Hauser, B.A., Cordonnier-Pratt, M.M., Nagatani, A., Koornneef, M., Pratt, L.H., and Kendrick, R.E. (1996). Molecular analysis of tri-mutant alleles in tomato indicates the Tri locus is the gene encoding the apoprotein of phytochrome B1. Planta **199**: 152–157.

Krueger, F. and Andrews, S.R. (2011). Bismark: A flexible aligner and methylation caller for Bisulfite-Seq applications. Bioinformatics **27**: 1571–1572.

Lang, Z., Wang, Y., Tang, K., Tang, D., Datsenka, T., Cheng, J., Zhang, Y., Handa, A.K., and Zhu, J.-K. (2017). Critical roles of DNA demethylation in the activation of ripening-induced genes and inhibition of ripening-repressed genes in tomato fruit. Proc. Natl. Acad. Sci. **114**: 4511–4519.

Lazarova, G.I., Kerckhoffs, L.H.J., Brandstädter, J., Matsui, M., Kendrick, R.E., Cordonnier-Pratt, M.M., and Pratt, L.H. (1998). Molecular analysis of PHYA in

wild-type and phytochrome A-deficient mutants of tomato. Plant J. **14**: 653–662.

Legris M., Klose C., Burgie E.S., Rojas C.C.R., Neme M., Hiltbrunner A., Wigge P.A., Schäfer E., Vierstra R.D., and Casal J.J. (2016). Phytochrome B integrates light and temperature signals in *Arabidopsis*. Science **354**: 897–900.

Lei, M., Zhang, H., Julian, R., Tang, K., Xie, S., and Zhu, J.-K. (2015). Regulatory link between DNA methylation and active demethylation in *Arabidopsis*. Proc. Natl. Acad. Sci. **112**: 3553–3557.

Li, Z., Jiang, G., Liu, X., Ding, X., Zhang, D., Wang, X., Zhou, Y., Yan, H., Li, T., Wu, K., Jiang, Y., and Duan, X. (2020). Histone demethylase SlJMJ6 promotes fruit ripening by removing H3K27 methylation of ripening-related genes in tomato. New Phytol. **227**: 1138–1156.

Lin, B.-Y., Shih, C.-J., Hsieh, H.-Y., Chen, H.-C., and Tu, S.-L. (2020). Phytochrome Coordinates with a hnRNP to Regulate Alternative Splicing via an Exonic Splicing Silencer. Plant Physiol. **182**: 243–254.

Lira, B.S., Gramegna, G., Trench, B.A., Alves, F.R.R., Silva, E.M., Silva, G.F.F., Thirumalaikumar, V.P., Lupi, A.C.D., Demarco, D., Purgatto, E., Nogueira, F.T.S., Balazadeh, S., Freschi, L., and Rossi, M. (2017). Manipulation of a senescence-associated gene improves fleshy fruit yield. Plant Physiol. **175**: 77–91.

Lister, R., O'Malley, R.C., Tonti-Filippini, J., Gregory, B.D., Berry, C.C., Millar, a. H., and Ecker, J.R. (2008). Highly Integrated Single-Base Resolution Maps of the Epigenome in *Arabidopsis*. Cell **133**: 523–536.

Liu, R., How-Kit A., Stammitti L., Teyssier E., Rolin D., Mortain-Bertrand A., Halle S., Liu M., Kong J., Wu C., Degraeve-Guibault C., Chapman N.H., Maucourt M., Hodgman T.C., Tost J., Bouzayen M., Hong Y., Seymour G.B., Giovannoni J.J., and Gallusci P. (2015). A DEMETER-like DNA demethylase governs tomato fruit ripening. Proc. Natl. Acad. Sci. **112**: 10804–10809.

Llorente B., D'Andrea L., Ruiz-Sola M.A., Botterweg E., Pulido P., Andilla J., Loza-Alvarez P., and Rodriguez-Concepcion M. (2016). Tomato fruit carotenoid biosynthesis is adjusted to actual ripening progression by a light-dependent mechanism. Plant J. **85**: 107–119.

Lu, X., Wang, W., Ren, W., Chai, Z., Guo, W., Chen, R., Wang, L., Zhao, J., Lang, Z., Fan, Y., Zhao, J., and Zhang, C. (2015). Genome-Wide Epigenetic Regulation of Gene Transcription in Maize Seeds. PLoS One **10**: e0139582.

Manning, K., Tör, M., Poole, M., Hong, Y., Thompson, A.J., King, G.J., Giovannoni, J.J., and Seymour, G.B. (2006). A naturally occurring epigenetic mutation in a gene encoding an SBP-box transcription factor inhibits tomato fruit ripening. Nat. Genet. **38**: 948–952.

Mazzella, M.A., Arana, M.V., Staneloni, R.J., Perelman, S., Rodríguez-Batiller, M.J., Muschietti, J., Cerdán, P.D., Chen, K., Sánchez, R.A., Zhu, T., Chory, J., and Casal, J.J. (2005). Phytochrome control of the *Arabidopsis* transcriptome anticipates seedling exposure to light. Plant Cell **17**: 2507–2516.

McCarthy, D.J., Chen, Y., and Smyth, G.K. (2012). Differential expression analysis of multifactor RNA-Seq experiments with respect to biological variation. Nucleic Acids Res. **40**: 4288–4297.

Omidvar, V. and Fellner, M. (2015). DNA Methylation and Transcriptomic Changes in Response to Different Lights and Stresses in 7B-1 Male-Sterile Tomato. PLoS One **10**: e0121864.

Paik, I. and Huq, E. (2019). Plant photoreceptors: Multi-functional sensory proteins and their signaling networks. Semin. Cell Dev. Biol. **92**: 114–121.

Perrella, G. and Kaiserli, E. (2016). Light behind the curtain: photoregulation of nuclear architecture and chromatin dynamics in plants. New Phytol. **212**: 908–919.

Pikaard, C.S. and Scheid, O.M. (2014). Epigenetic regulation in plants. Cold Spring Harb. Perspect. Biol. **6**: 1–32.

Pontvianne, F., Blevins, T., and Pikaard, C.S. (2010). *Arabidopsis* Histone Lysine Methyltransferases. **53**: 1–22.

Robinson, M.D., McCarthy, D.J., and Smyth, G.K. (2009). edgeR: a Bioconductor package for differential expression analysis of digital gene expression data. Bioinformatics **26**: 139–140.

Shikata, H., Hanada, K., Ushijima, T., Nakashima, M., Suzuki, Y., and Matsushita, T. (2014). Phytochrome controls alternative splicing to mediate light responses in *Arabidopsis*. Proc. Natl. Acad. Sci. U. S. A. **111**: 18781–18786.

Tessadori, F., van Zanten M., Pavlova P., Clifton R., Pontvianne F., Snoek L.B., Millenaar F.F., Schulkes R.K., van Driel R., Voesenek L.A., Spillane C., Pikaard C.S., Fransz P., and Peeters AJ. (2009). Phytochrome B and histone deacetylase 6 control light-induced chromatin compaction in *Arabidopsis thaliana*. PLoS Genet. **5**: e1000638.

Thimm, O., Bläsing, O., Gibon, Y., Nagel, A., Meyer, S., Krüger, P., Selbig, J., Müller, L.A., Rhee, S.Y., and Stitt, M. (2004). mapman: a user-driven tool to display genomics data sets onto diagrams of metabolic pathways and other biological processes. Plant J. **37**: 914–939.

Ushijima, T., Hanada K., Gotoh E., Yamori W., Kodama Y., Tanaka H., Kusano M., Fukushima A., Tokizawa M., Yamamoto Y.Y., Tada Y., Suzuki Y., and Matsushita T. (2017). Light Controls Protein Localization through Phytochrome-Mediated Alternative Promoter Selection. Cell **171**: 1316-1325.

Vrebalov, J., Ruezinsky, D., Padmanabhan, V., White, R., Medrano, D., Drake, R., Schuch, W., and Giovannoni, J. (2002). A MADS-Box Gene Necessary for Fruit Ripening at the tomato *ripening-inhinitor* (*rin*) locus. Science. **296**: 343–346.

Wu, H.-P., Su, Y., Chen, H.-C., Chen, Y.-R., Wu, C.-C., Lin, W.-D., and Tu, S.-L. (2014). Genome-wide analysis of light-regulated alternative splicing mediated by photoreceptors in *Physcomitrella patens*. Genome Biol. **15**: R10.

Zemach, A., Kim, M.Y., Hsieh, P.H., Coleman-Derr, D., Eshed-Williams, L., Thao, K., Harmer, S.L., and Zilberman, D. (2013). The *Arabidopsis* nucleosome remodeler DDM1 allows DNA methyltransferases to access H1-containing heterochromatin. Cell **153**: 193–205.

Zhang, B., Tieman, D.M., Jiao, C., Xu, Y., Chen, K., Fei, Z., Giovannoni, J.J., and Klee, H.J. (2016). Chilling-induced tomato flavor loss is associated with altered volatile synthesis and transient changes in DNA methylation. Proc. Natl. Acad. Sci. **113**: 12580–12585.

Zhang, H., Lang, Z., and Zhu, J.K. (2018). Dynamics and function of DNA methylation in plants. Nat. Rev. Mol. Cell Biol. **19**: 489–506.

Zhang, Y., Liu, T., Meyer, C.A., Eeckhoute, J., Johnson, D.S., Bernstein, B.E., Nusbaum, C., Myers, R.M., Brown, M., Li, W., and Liu, X.S. (2008). Model-based

Analysis of ChIP-Seq (MACS). Genome Biol. **9**: R137.

Zhang, Y., Mayba, O., Pfeiffer, A., Shi, H., Tepperman, J.M., Speed, T.P., and Quail, P.H. (2013). A Quartet of PIF bHLH Factors Provides a Transcriptionally Centered Signaling Hub That Regulates Seedling Morphogenesis through Differential Expression-Patterning of Shared Target Genes in *Arabidopsis*. PLOS Genet. **9**: e1003244.

Zhao, L., Lu, J., Zhang, J., Wu, P.-Y., Yang, S., and Wu, K. (2015). Identification and characterization of histone deacetylases in tomato (*Solanum lycopersicum*) . Front. Plant Sci. **5**: 760.

Zhong, S., Fei, Z., Chen, Y.R., Zheng, Y., Huang, M., Vrebalov, J., McQuinn, R., Gapper, N., Liu, B., Xiang, J., Shao, Y., and Giovannoni, J.J. (2013). Single-base resolution methylomes of tomato fruit development reveal epigenome modifications associated with ripening. Nat. Biotechnol. **31**: 154–159.

Zuo, J., Grierson, D., Courtney, L.T., Wang, Y., Gao, L., Zhao, X., Zhu, B., Luo, Y., Wang, Q., and Giovannoni, J.J. (2020). Relationships between genome methylation, levels of non-coding RNAs, mRNAs and metabolites in ripening tomato fruit. Plant J. **103**: 980-994.

Figure legends

Figure 1. PHYA and PHYB1B2 modify the global transcriptomic profile of tomato fruit. (A) Number of differentially expressed genes (DEGs) in *phyA* and *phyB1B2* mutant fruits at immature green (IG) and breaker (BK) stages. (B) Venn diagram showing exclusive and common DEGs in *phyA* and *phyB1B2* mutants in both developmental stages. (C) Functional categorization of all DEGs and those DEGs with differentially methylated promoters (DMPs) in both analysed genotypes and stages. Only categories corresponding to at least 2% of the DEGs or DMPs in each comparison are shown (asterisks). Up- and downregulated genes are indicated in red and blue, respectively. Loci with hyper- and hypomethylated promoters are indicated in light red and light blue, respectively. DEGs and DMPs show statistically significant differences (FDR < 0.05) relative to WT.

Figure 2. Disturbed PHYA- and PHYB1B2-dependent signalling differentially alters tomato fruit methylome. (A) Density plot of genes, transposable elements (TEs) and mC in all

contexts (mCG, mCHG, mCHH) for the WT genotype. Global methylation changes for *phyA* and *phyB1B2* in comparison with the wild type (WT) at the immature green (IG) and breaker (BK) stages are shown (bin size, 1 Mb). Gene and TE densities were estimated according to the number of nucleotides covered per million. The methylation levels in the CG, CHG and CHH contexts are 40-90%, 25-80% and 10-30%, respectively. The mC difference was relative to the corresponding WT fruit stage within a -5% (hypomethylated) ≤ range ≤ +5% (hypermethylated). (B) Number of genes with differentially methylated promoters (DMPs, 2 kb upstream transcription start site) in *phyA*, *phyB1B2* and both mutants. Hyper- and hypomethylation are indicated by grey and darker-coloured bars, respectively. DMPs show statistically significant differences (FDR < 0.05) relative to WT.

Figure 3. Phytochrome deficiency impacts the sRNAome profile. (A) Total number of differentially methylated sRNA cluster-targeted genome regions (sCTGRs). (B) Scatter plots show the relationship between the differential accumulation of cluster sRNAs and a minimum of 5% differential methylation of their sCTGRs. The result of Fischer´s test for the association of the two datasets is shown ($p \leq 2.07e^{-5}$). (C) Boxplots show changes in the accumulation of cluster sRNAs in promoter (P, 2 Kb upstream of the 5' UTR end) and gene body (GB) regions for up- and downregulated DEGs. Asterisks indicate statistically significant differences by the Wilcoxon–Mann–Whitney test (** $p<0.0001$). All results represent the comparison of *phyA* and *phyB1B2* to the wild type in immature green (IG) and breaker (BK) fruit stages.

Figure 4. Methylation across promoter and gene body regions differentially affects gene expression. (A) Relative expression of *RIPENING INHIBITOR* (*RIN*) and *FRUITFULL 2* (*FUL2*) in immature green (IG) and mature green (MG) fruits from *phyB1B2* determined by RT-qPCR. Red dots indicate data from RNA-seq in the same stage. Expression levels represent the mean of at least three biological replicates and are relative to the wild type (WT). Asterisks indicate statistically significant differences by the two-tailed Student´s *t* test compared to WT (* $p<0.05$). (B) Differential gene body methylation (green bars) and sRNA accumulation (black bars) within *RIN* and *FUL2* in IG fruits from the *phyB1B2* and WT genotypes.

Figure 5. PHYB1/B2-dependent methylation regulates fruit chlorophyll. (A) Relative content of total chlorophyll in IG fruits from *phyB1B2* and WT genotypes. Values represent

the mean of at least three biological replicates. Asterisks indicate statistically significant differences by the two-tailed Student's *t* test between genotypes (** $p<0.01$). (B) Relative expression of *CHLOROPHYLL A/B BINDING PROTEINs* (*CBP* and *CAB-3c*) and *PROTOCHLOROPHYLLIDE OXIDOREDUCTASE 3* (*POR3*) in IG fruits from *phyB1B2* determined by RNA-seq. Expression levels represent the mean of at least three biological replicates and are relative to WT. Asterisks indicate statistically significant differences compared to WT (* FDR≤0.05). (C) Differential promoter methylation in *CBP*, *CAB-3c* and *POR3* in IG fruits from the *phyB1B2* and WT genotypes. HY5 and PIF transcription factor binding motifs are denoted with arrows.

Figure 6. PHYB1/B2 influence on fruit ripening is associated to the promoter demethylation of master ripening-associated transcription factors (A) Differentially methylated promoters of the *RIPENING INHIBITOR* (*RIN*), *NON-RIPENING* (*NOR*), *COLORLESS NORIPENING* (*CNR*) and *APETALA 2a* (*AP2a*) loci between the *phyB1B2* and wild-type (WT) genotypes. Green and orange indicate total mC in immature green (IG) and breaker (BK) fruits, respectively. HY5 and PIF transcription factor binding motifs are denoted with arrows. Thick blue lines indicate RIN binding sites according to ChIP-seq data (Zhong et al., 2013). (B) Relative expression from the RT-qPCR assay of genes encoding master ripening transcription factors in BK and red ripe (RR) fruits from *phyB1B2*. Red dots indicate data from RNA-seq in the same stage. Expression levels represent the mean of at least three biological replicates and are relative to WT. Asterisks indicate statistically significant differences by two-tailed Student's *t* test compared to WT (* $p<0.05$).

Figure 7. PHYB1/B2-dependent regulation of fruit carotenogenesis relies on the promoter demethylation of key carotenoid biosynthetic genes. (A) Relative contents of total carotenoids in red ripe (RR) fruits from phyB1B2 and wild-type (WT) genotypes. Values represent the mean of at least three biological replicates. Asterisks indicate statistically significant differences by the two-tailed Student's *t* test between genotypes (** $p<0.01$). (B) Differentially methylated promoter sites of the *PHYTOENE SYNTHASE 1* (*PSY1*), *PHYTOENE DESATURASE* (*PDS*), *15-CIS- ζ-CAROTENE* (*ZISO*) and *ZETA-CAROTENE DESATURASE* (*ZDS*) loci between the *phyB1B2* and WT genotypes. Orange colour indicates total mC in breaker (BK) fruits. Arrows denote HY5 and PIF transcription factor binding motifs. Thick blue lines indicate RIN binding sites according to ChIP-seq data (Zhong et al.,

2013). (C) Relative expression of carotenoid biosynthetic enzyme-encoding genes in immature green (IG), mature green (MG), BK and RR fruits from *phyB1B2* determined by RT-qPCR. Red dots indicate data from RNA-seq in the same stage. The expression levels represent the mean of at least three biological replicates and are relative to WT. Asterisks indicate statistically significant differences by the two-tailed Student's *t* test compared to WT (*$p<0.05$, ** $p<0.01$).

Figure 8. Model of epigenetic mechanisms involved in fruit development regulation triggered by PHYB1B2. (A) PHYB1B2 contributes to the reciprocal regulation between HDT3 and RIN through the inhibition and induction of *HDT3* and *RIN* expression, respectively. Increases in *RIN* expression during fruit maturation inhibit *HDT3* levels triggering DNA demethylation and consequently fruit ripening. (B) Active PHYB1B2 regulates the expression of genes associated with DNA methylation (*MET1L*), chromatin remodelling (*DDM1*) and histone modifiers (*PRMT* and *HDT3*), promoting overall fruit DNA demethylation during the ripening process. PHYB1B2-mediated methylation reprogramming results in the upregulation of master TFs, which in turn trigger ripening and carotenogenesis.

Supplemental Figure 1. Global methylation status in *phyA*, *phyB1B2* and WT at IG and BK stage for mCG (a), mCHG (b) and mCHH (c) contexts. Density plot ofgenes, transposable elements (TEs) and sRNAs clusters were estimated by the number of nucleotides covered per million. Methylation levels for CG, CHG and CHHcontexts, are 40-90%; 25-80% and 10-30%, respectively. Cytosine density for CG, CHG and CHH contexts, are 0 - 17,488; 0 - 13,105 and 0 - 103,903 per million,respectively.

Supplemental Figure 2. mRNA level alterations associated with differences in the promoter methylation in*phyA* and *phyB1B2* compared to WT. Scatter plots show the DEGs that showed DMPs at immature green(IG) and breaker (BK) fruit stages, the axes indicate the variation between both parameters compared to WT(DEGs, FDR < 0.05; DMPs, FDR < 0.05) in CG, CHG and CHH contexts. Only DMPs with changes inmethylation levels > 5% are shown.

Supplemental Figure 3. Comparison of the association of DMPs and DEGs between immature green andbreaker stages within each genotype. DMPs: differentially methylated promoters; DEGs: differentially expressed genes.

Supplemental Figure 4. Methylation levels in sRNA cluster targeted genomic region (sCTGR) and small RNA accumulation changes between IG and BK stages in WT, *phyA* and *phyB1B2* genotypes. Scatter plots show the relationship between the small RNA accumulation and differential methylation on their target genomic regions between immature green (IG) and breaker (BK) fruit stages.

Supplemental Figure 5. RIN motif *de novo* discovered using MEME algorithm. Consensus sequence CCWWWWWWGG (CC(6W)GG) and extended TTWCCWWWWWWGGWAA length=16.

Supplemental Figure 6. DMP sites in the *ROS1L* locus in WT and *phyB1B2* BK fruits. Red rectangles indicate the presence of transposable element (TE).

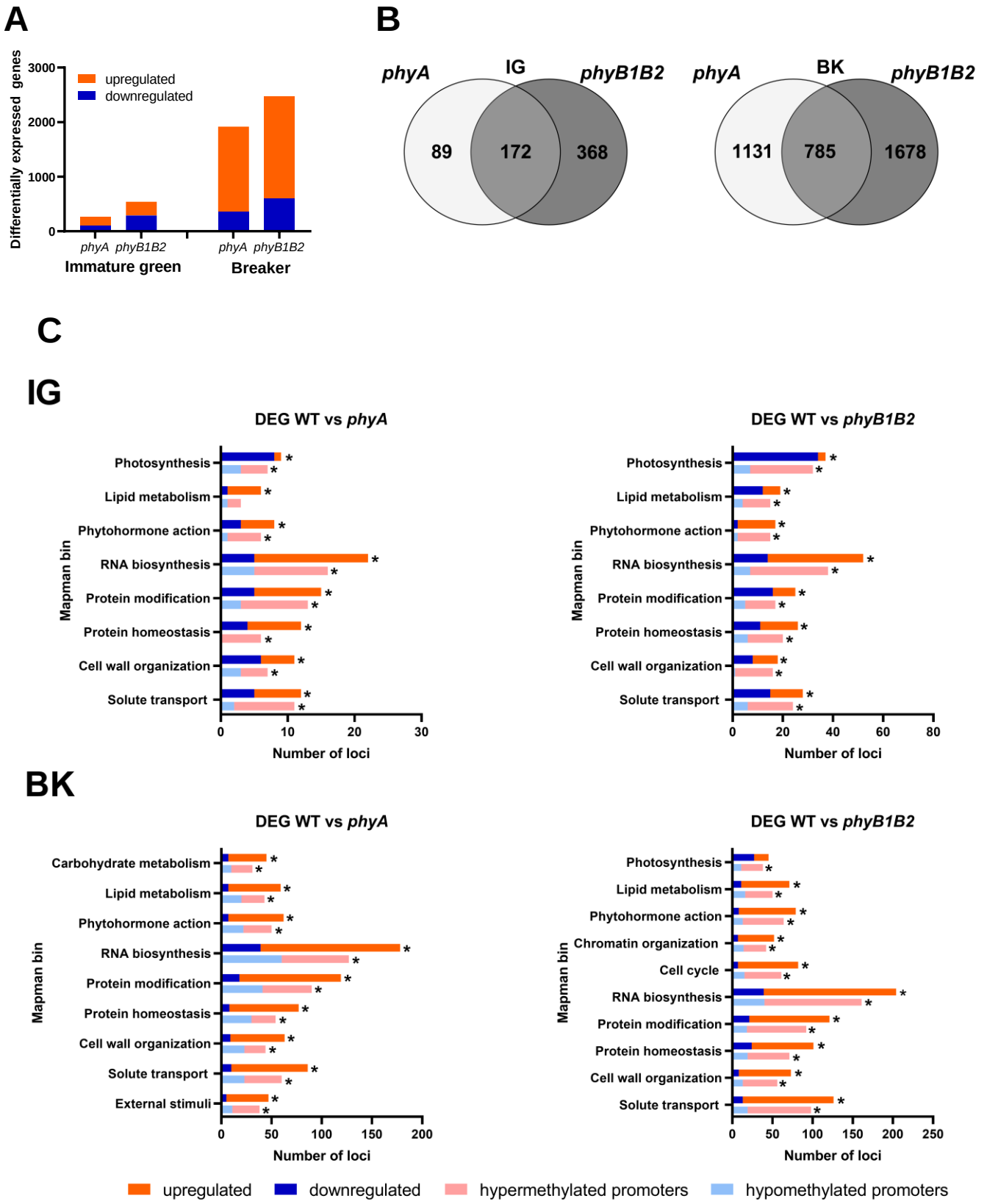
A
Differentially expressed genes
3000
2000
1000
0
upregulated
downregulated
phyA
phyB1B2
phyA
phyB1B2
Immature green
Breaker
B
phyA
IG
phyB1B2
89
172
368
phyA
BK
phyB1B2
1131
785
1678
C
IG
DEG WT vs phyA
Mapman bin
Photosynthesis
Lipid metabolism
Phytohormone action
RNA biosynthesis
Protein modification
Protein homeostasis
Cell wall organization
Solute transport
Number of loci
DEG WT vs phyB1B2
Mapman bin
Photosynthesis
Lipid metabolism
Phytohormone action
RNA biosynthesis
Protein modification
Protein homeostasis
Cell wall organization
Solute transport
Number of loci
BK
DEG WT vs phyA
Mapman bin
Carbohydrate metabolism
Lipid metabolism
Phytohormone action
RNA biosynthesis
Protein modification
Protein homeostasis
Cell wall organization
Solute transport
External stimuli
Number of loci
DEG WT vs phyB1B2
Mapman bin
Photosynthesis
Lipid metabolism
Phytohormone action
Chromatin organization
Cell cycle
RNA biosynthesis
Protein modification
Protein homeostasis
Cell wall organization
Solute transport
Number of loci
upregulated
downregulated
hypermethylated promoters
hypomethylated promoters

Figure 1. PHYA and PHYB1B2 modify the global transcriptomic profile of tomato fruit. (A) Number of differentially expressed genes (DEGs) in *phyA* and *phyB1B2* mutant fruits at immature green (IG) and breaker (BK) stages. (B) Venn diagram showing exclusive and common DEGs in *phyA* and *phyB1B2* mutants in both developmental stages. (C) Functional categorization of all DEGs and those DEGs with differentially methylated promoters (DMPs) in both analysed genotypes and stages. Only categories corresponding to at least 2% of the DEGs or DMPs in each comparison are shown (asterisks). Up- and downregulated genes are indicated in red and blue, respectively. Loci with hyper- and hypomethylated promoters are indicated in light red and light blue, respectively. DEGs and DMPs show statistically significant differences (FDR < 0.05) relative to WT.

A

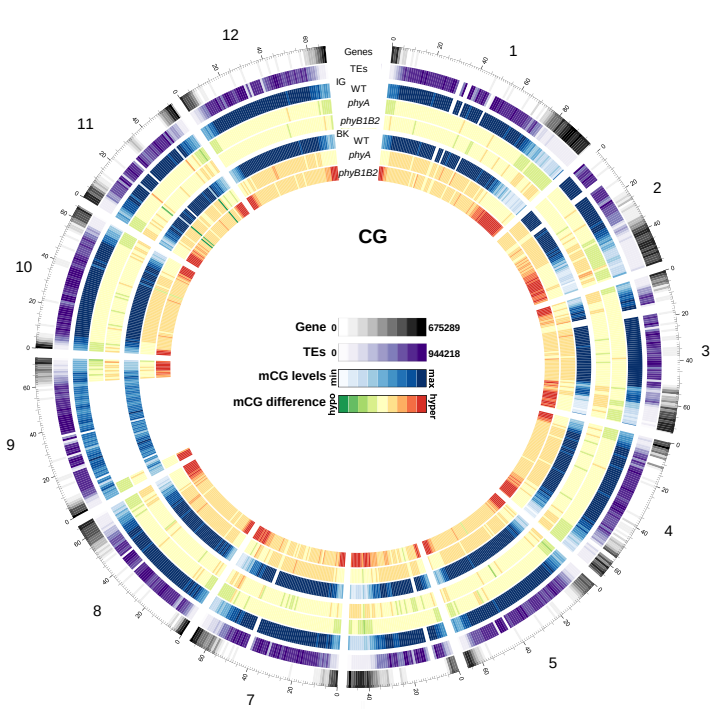
CG
Genes
TEs
IG
WT
phyA
phyB1B2
BK
WT
phyA
phyB1B2
Gene 0
675289
TEs 0
944218
mCG levels
min
max
mCG difference
hypo
hyper
1
2
3
4
5
6
7
8
9
10
11
12

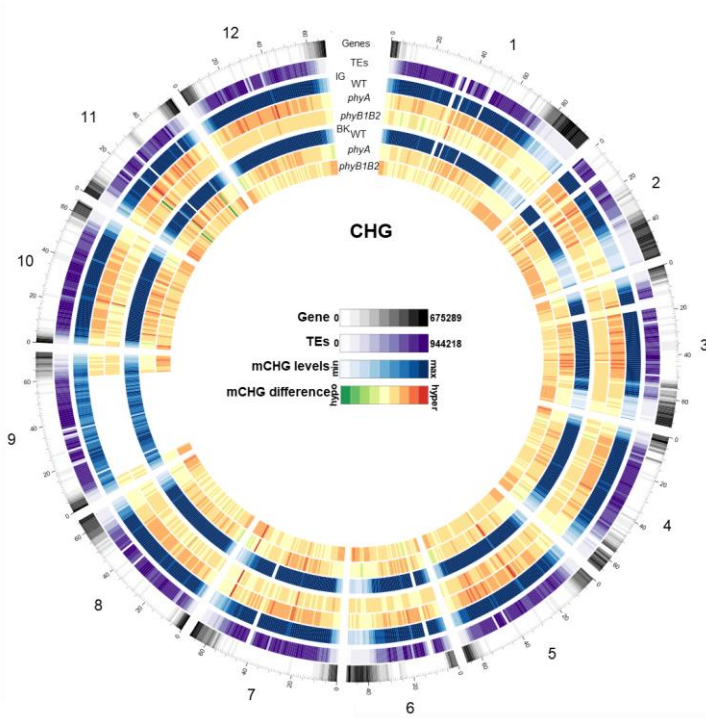
CHG
Genes
TEs
IG
WT
phyA
phyB1B2
BK
WT
phyA
phyB1B2
Gene 0
675289
TEs 0
944218
mCHG levels
min
max
mCHG difference
hypo
hyper
1
2
3
4
5
6
7
8
9
10
11
12

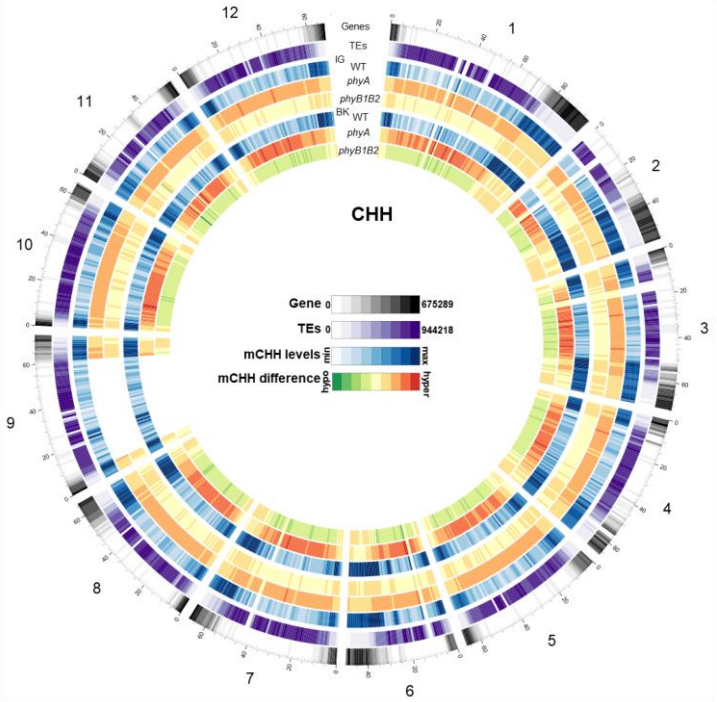
CHH
Genes
TEs
IG
WT
phyA
phyB1B2
BK
WT
phyA
phyB1B2
Gene 0
675289
TEs 0
944218
mCHH levels
min
max
mCHH difference
hypo
hyper
1
2
3
4
5
6
7
8
9
10
11
12

B

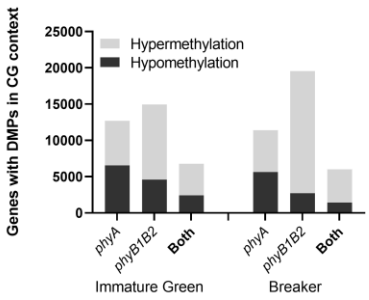
CG
Genes with DMPs in CG context
Hypermethylation
Hypomethylation
25000
20000
15000
10000
5000
0
phyA
phyB1B2
Both
phyA
phyB1B2
Both
Immature Green
Breaker

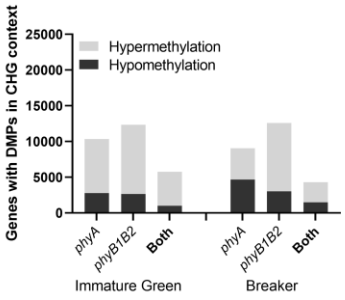
CHG
Genes with DMPs in CHG context
Hypermethylation
Hypomethylation
25000
20000
15000
10000
5000
0
phyA
phyB1B2
Both
phyA
phyB1B2
Both
Immature Green
Breaker

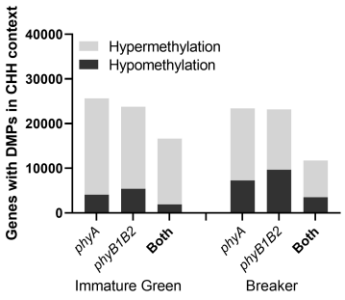
CHH
Genes with DMPs in CHH context
Hypermethylation
Hypomethylation
40000
30000
20000
10000
0
phyA
phyB1B2
Both
phyA
phyB1B2
Both
Immature Green
Breaker

Figure 2. Disturbed PHYA- and PHYB1B2-dependent signalling differentially alters tomato fruit methylome. (A) Density plot of genes, transposable elements (TEs) and mC in all contexts (mCG, mCHG, mCHH) for the WT genotype. Global methylation changes for *phyA* and *phyB1B2* in comparison with the wild type (WT) at the immature green (IG) and breaker (BK) stages are shown (bin size, 1 Mb). Gene and TE densities were estimated according to the number of nucleotides covered per million. The methylation levels in the CG, CHG and CHH contexts are 40-90%, 25-80% and 10-30%, respectively. The mC difference was relative to the corresponding WT fruit stage within a -5% (hypomethylated) ≤ range ≤ +5% (hypermethylated). (B) Number of genes with differentially methylated promoters (DMPs, 2 kb upstream transcription start site) in *phyA*, *phyB1B2* and both mutants. Hyper- and hypomethylation are indicated by grey and darker-coloured bars, respectively. DMPs show statistically significant differences (FDR < 0.05) relative to WT.

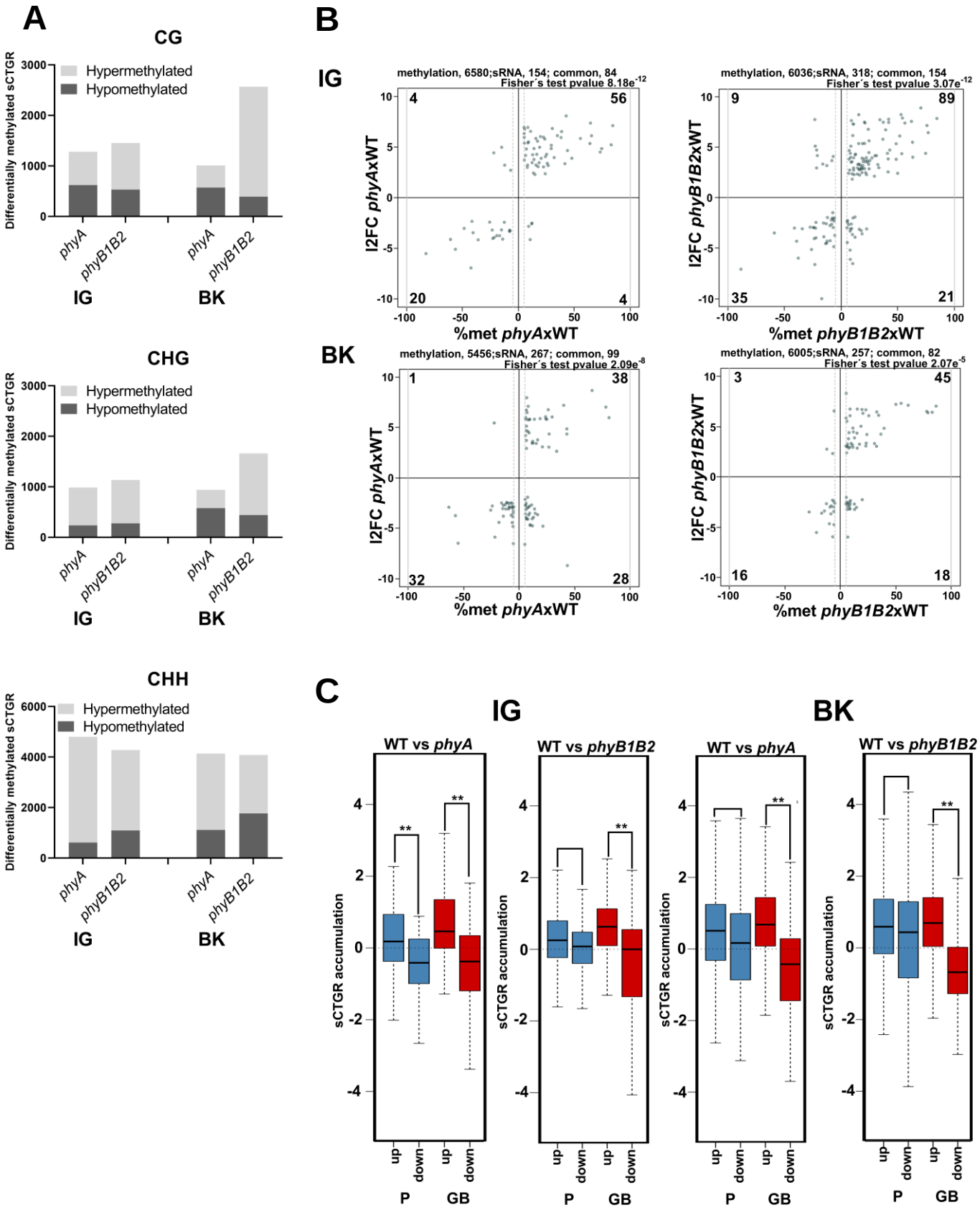
A
CG
Hypermethylated
Hypomethylated
Differentially methylated sCTGR
phyA
phyB1B2
IG
BK
CHG
CHH
B
IG
methylation, 6580;sRNA, 154; common, 84
Fisher´s test pvalue 8.18e-12
methylation, 6036;sRNA, 318; common, 154
Fisher´s test pvalue 3.07e-12
BK
methylation, 5456;sRNA, 267; common, 99
Fisher´s test pvalue 2.09e-8
methylation, 6005;sRNA, 257; common, 82
Fisher´s test pvalue 2.07e-5
l2FC phyAxWT
l2FC phyB1B2xWT
%met phyAxWT
%met phyB1B2xWT
C
IG
BK
WT vs phyA
WT vs phyB1B2
sCTGR accumulation
up
down
P
GB

Figure 3. Phytochrome deficiency impacts the sRNAome profile. (A) Total number of differentially methylated sRNA cluster-targeted genome regions (sCTGRs). (B) Scatter plots show the relationship between the differential accumulation of cluster sRNAs and a minimum of 5% differential methylation of their sCTGRs. The result of Fischer´s test for the association of the two datasets is shown ($p \leq 2.07e^{-5}$). (C) Boxplots show changes in the accumulation of cluster sRNAs in promoter (P, 2 Kb upstream of the 5' UTR end) and gene body (GB) regions for up- and downregulated DEGs. Asterisks indicate statistically significant differences by the Wilcoxon–Mann–Whitney test (** $p<0.0001$). All results represent the comparison of *phyA* and *phyB1B2* to the wild type in immature green (IG) and breaker (BK) fruit stages.

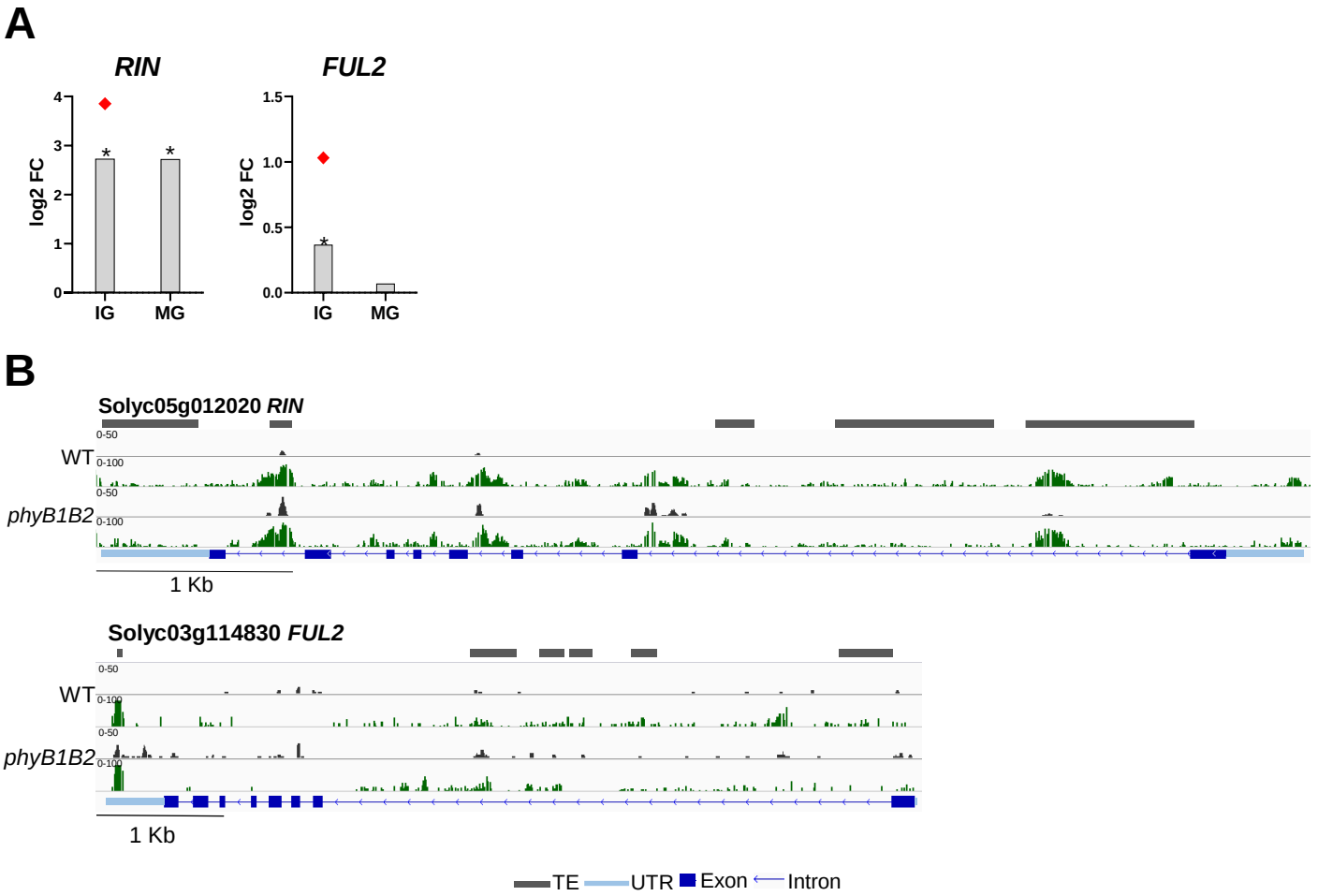

Figure 4. Methylation across promoter and gene body regions differentially affects gene expression. (A) Relative expression of *RIPENING INHIBITOR* (*RIN*) and *FRUITFULL 2* (*FUL2*) in immature green (IG) and mature green (MG) fruits from *phyB1B2* determined by RT-qPCR. Red dots indicate data from RNA-seq in the same stage. Expression levels represent the mean of at least three biological replicates and are relative to the wild type (WT). Asterisks indicate statistically significant differences by the two-tailed Student´s *t* test compared to WT (* $p<0.05$). (B) Differential gene body methylation (green bars) and sRNA accumulation (black bars) within *RIN* and *FUL2* in IG fruits from the *phyB1B2* and WT genotypes.

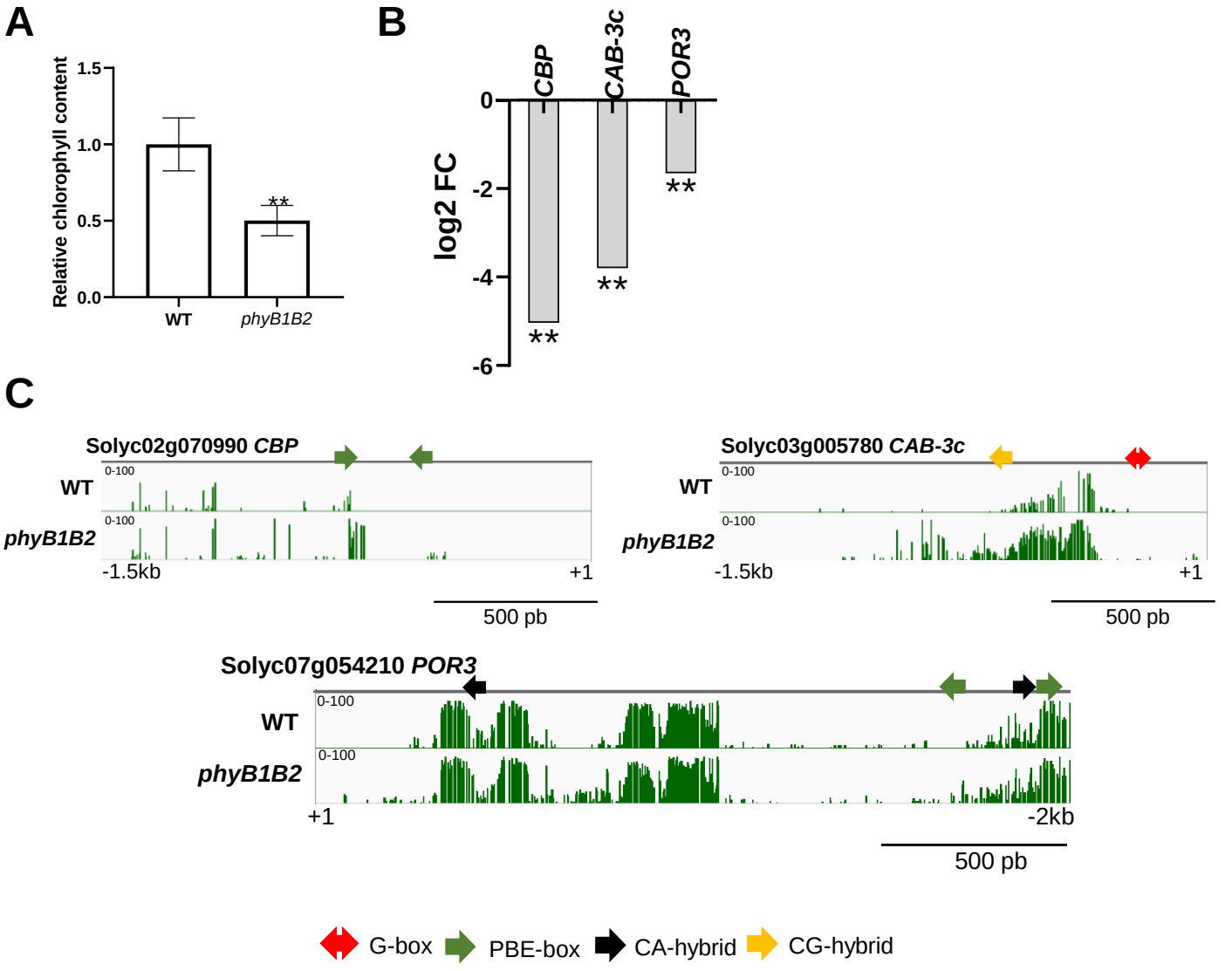
A
Relative chlorophyll content
1.5
1.0
0.5
0.0
**
WT
phyB1B2
B
log2 FC
0
-2
-4
-6
CBP
CAB-3c
POR3
**
**
**
C
Solyc02g070990 CBP
WT
phyB1B2
0-100
0-100
-1.5kb
+1
500 pb
Solyc03g005780 CAB-3c
WT
phyB1B2
0-100
0-100
-1.5kb
+1
500 pb
Solyc07g054210 POR3
WT
phyB1B2
0-100
0-100
+1
-2kb
500 pb
G-box
PBE-box
CA-hybrid
CG-hybrid

Figure 5. PHYB1/B2-dependent methylation regulates fruit chlorophyll. (A) Relative content of total chlorophyll in IG fruits from *phyB1B2* and WT genotypes. Values represent the mean of at least three biological replicates. Asterisks indicate statistically significant differences by the two-tailed Student's *t* test between genotypes (** $p<0.01$). (B) Relative expression of *CHLOROPHYLL A/B BINDING PROTEINs* (*CBP* and *CAB-3c*) and *PROTOCHLOROPHYLLIDE OXIDOREDUCTASE 3* (*POR3*) in IG fruits from *phyB1B2* determined by RNA-seq. Expression levels represent the mean of at least three biological replicates and are relative to WT. Asterisks indicate statistically significant differences compared to WT (* FDR≤0.05). (C) Differential promoter methylation in *CBP*, *CAB-3c* and *POR3* in IG fruits from the *phyB1B2* and WT genotypes. HY5 and PIF transcription factor binding motifs are denoted with arrows.

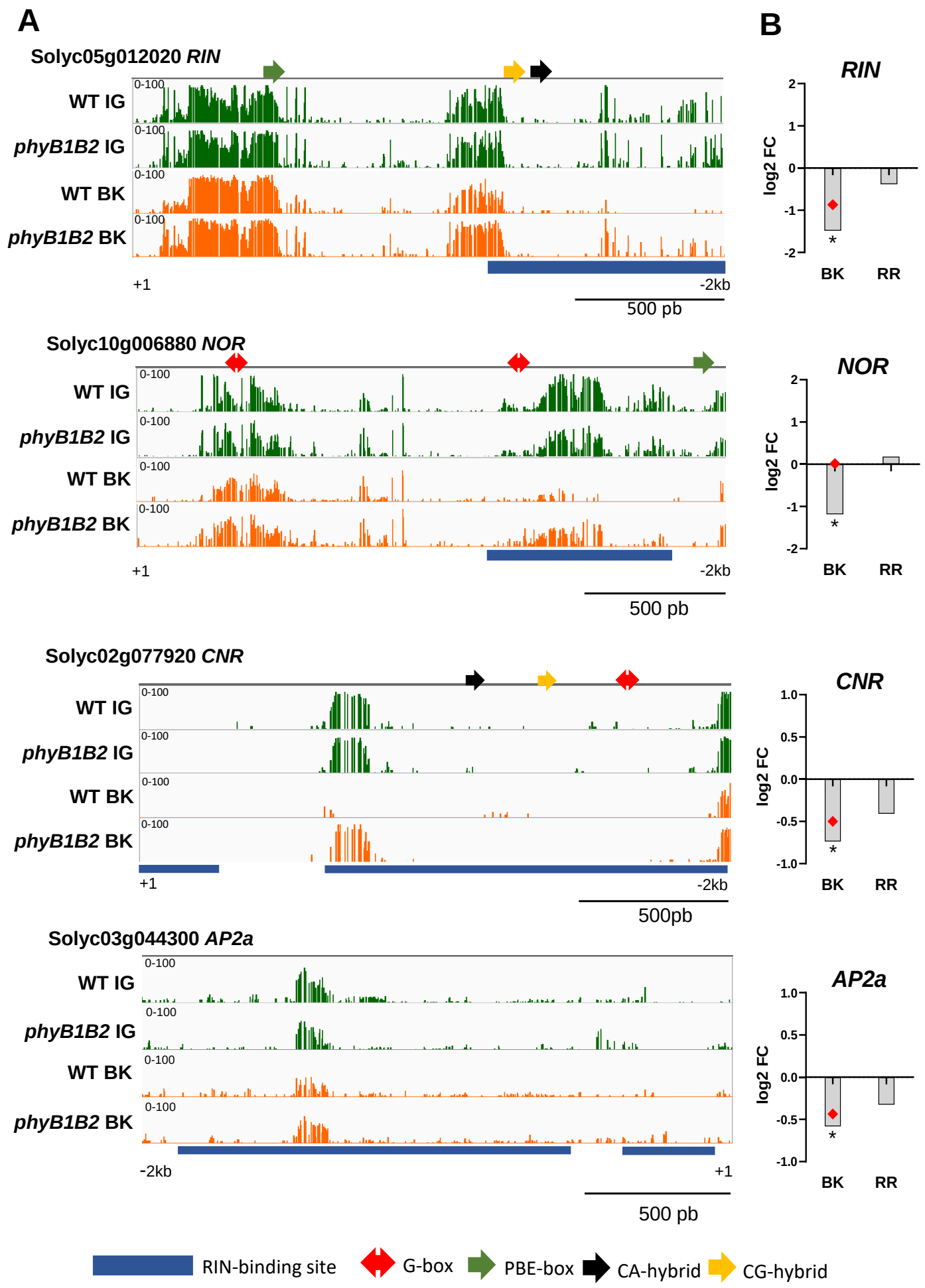
A
B
Solyc05g012020 RIN
WT IG
phyB1B2 IG
WT BK
phyB1B2 BK
0-100
+1
-2kb
500 pb
RIN
log2 FC
BK
RR
Solyc10g006880 NOR
NOR
Solyc02g077920 CNR
CNR
500pb
Solyc03g044300 AP2a
AP2a
RIN-binding site
G-box
PBE-box
CA-hybrid
CG-hybrid

Figure 6. PHYB1/B2 influence on fruit ripening is associated to the promoter demethylation of master ripening-associated transcription factors. (A) Differentially methylated promoters of the *RIPENING INHIBITOR* (*RIN*), *NON-RIPENING* (*NOR*), *COLORLESS NORIPENING* (*CNR*) and *APETALA 2a* (*AP2a*) loci between the *phyB1B2* and wild-type (WT) genotypes. Green and orange indicate total mC in immature green (IG) and breaker (BK) fruits, respectively. HY5 and PIF transcription factor binding motifs are denoted with arrows. Thick blue lines indicate RIN binding sites according to ChIP-seq data (Zhong et al., 2013). (B) Relative expression from the RT-qPCR assay of genes encoding master ripening transcription factors in BK and red ripe (RR) fruits from *phyB1B2*. Red dots indicate data from RNA-seq in the same stage. Expression levels represent the mean of at least three biological replicates and are relative to WT. Asterisks indicate statistically significant differences by two-tailed Student's *t* test compared to WT (* $p<0.05$).

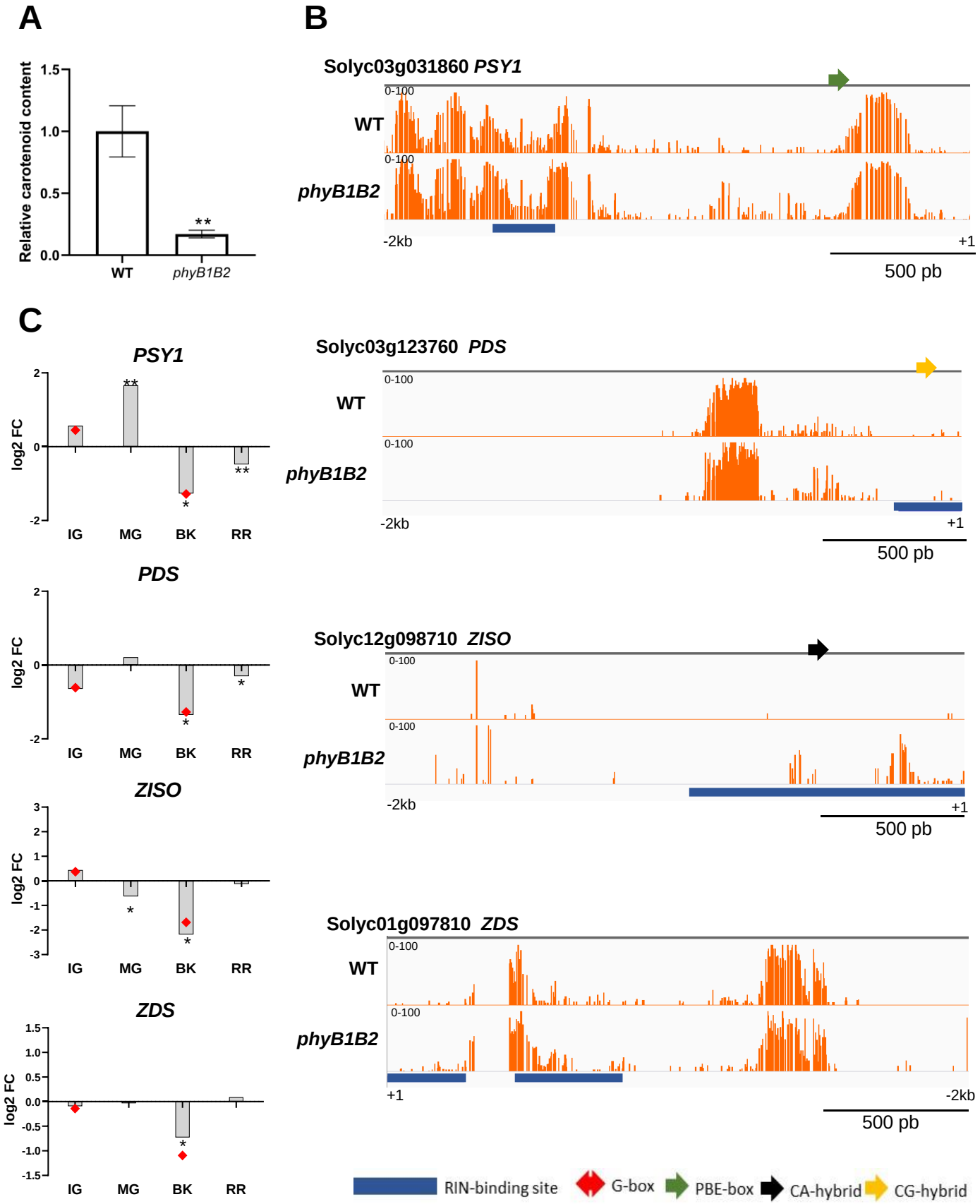
A
Relative carotenoid content
1.5
1.0
0.5
0.0
**
WT
phyB1B2
B
Solyc03g031860 PSY1
WT
phyB1B2
0-100
0-100
-2kb
+1
500 pb
Solyc03g123760 PDS
WT
phyB1B2
0-100
0-100
-2kb
+1
500 pb
Solyc12g098710 ZISO
WT
phyB1B2
0-100
0-100
-2kb
+1
500 pb
Solyc01g097810 ZDS
WT
phyB1B2
0-100
0-100
+1
-2kb
500 pb
C
PSY1
PDS
ZISO
ZDS
log2 FC
IG
MG
BK
RR
RIN-binding site
G-box
PBE-box
CA-hybrid
CG-hybrid

Figure 7. PHYB1/B2-dependent regulation of fruit carotenogenesis relies on the promoter demethylation of key carotenoid biosynthetic genes. (A) Relative contents of total carotenoids in red ripe (RR) fruits from phyB1B2 and wild-type (WT) genotypes. Values represent the mean of at least three biological replicates. Asterisks indicate statistically significant differences by the two-tailed Student's *t* test between genotypes (** $p<0.01$). (B) Differentially methylated promoter sites of the *PHYTOENE SYNTHASE 1* (*PSY1*), *PHYTOENE DESATURASE* (*PDS*), *15-CIS- ζ-CAROTENE* (*ZISO*) and *ZETA-CAROTENE DESATURASE* (*ZDS*) loci between the *phyB1B2* and WT genotypes. Orange colour indicates total mC in breaker (BK) fruits. Arrows denote HY5 and PIF transcription factor binding motifs. Thick blue lines indicate RIN binding sites according to ChIP-seq data (Zhong et al., 2013). (C) Relative expression of carotenoid biosynthetic enzyme-encoding genes in immature green (IG), mature green (MG), BK and RR fruits from *phyB1B2* determined by RT-qPCR. Red dots indicate data from RNA-seq in the same stage. The expression levels represent the mean of at least three biological replicates and are relative to WT. Asterisks indicate statistically significant differences by the two-tailed Student's *t* test compared to WT (*$p<0.05$, ** $p<0.01$).

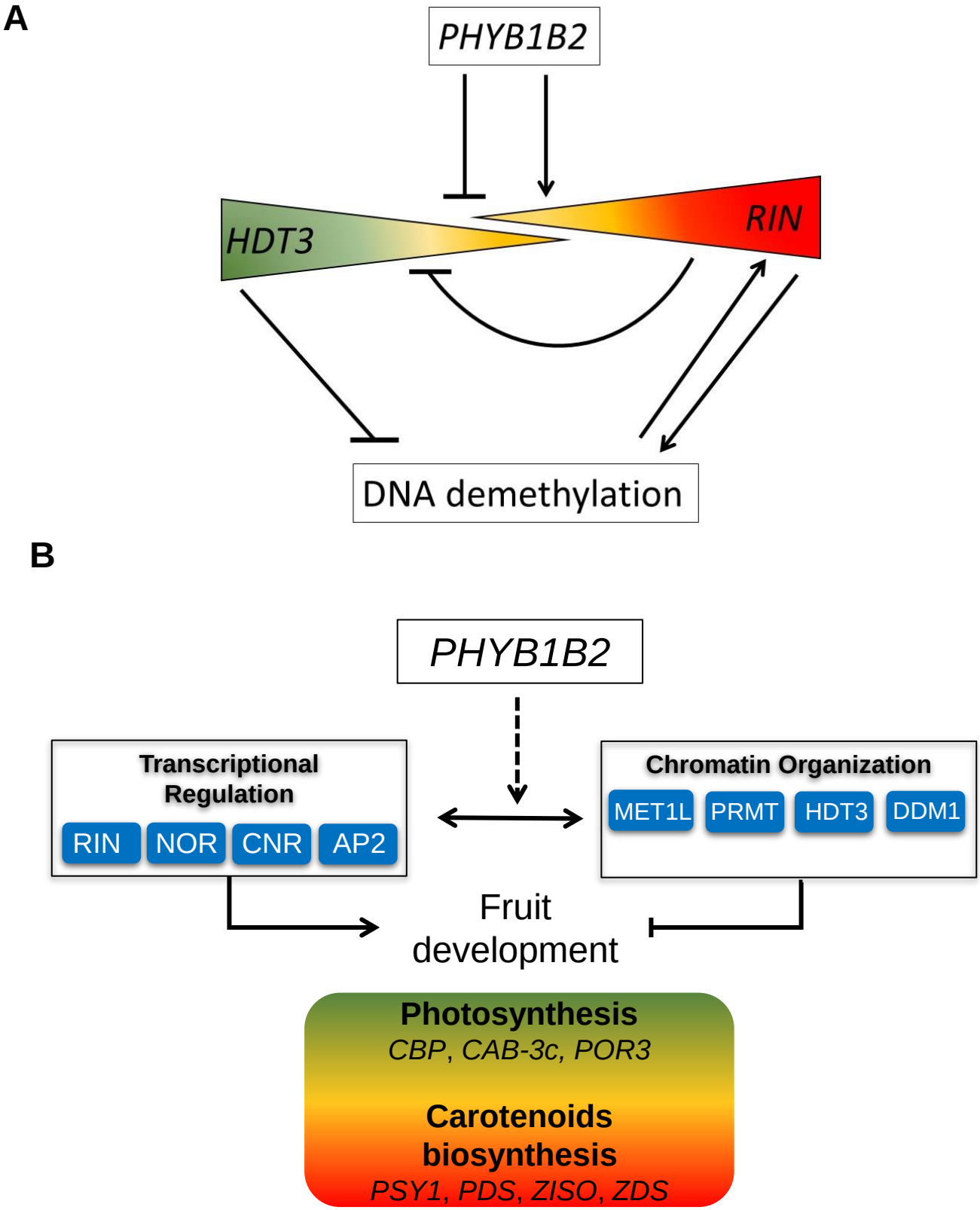
A
PHYB1B2
HDT3
RIN
DNA demethylation
B
PHYB1B2
Transcriptional Regulation
RIN
NOR
CNR
AP2
Chromatin Organization
MET1L
PRMT
HDT3
DDM1
Fruit development
Photosynthesis
CBP, CAB-3c, POR3
Carotenoids biosynthesis
PSY1, PDS, ZISO, ZDS

Figure 8. Model of epigenetic mechanisms involved in fruit development regulation triggered by PHYB1B2. (A) PHYB1B2 contributes to the reciprocal regulation between HDT3 and RIN through the inhibition and induction of *HDT3* and *RIN* expression, respectively. Increases in *RIN* expression during fruit maturation inhibit *HDT3* levels triggering DNA demethylation and consequently fruit ripening. (B) Active PHYB1B2 regulates the expression of genes associated with DNA methylation (*MET1L*), chromatin remodelling (*DDM1*) and histone modifiers (*PRMT* and *HDT3*), promoting overall fruit DNA demethylation during the ripening process. PHYB1B2-mediated methylation reprogramming results in the upregulation of master TFs, which in turn trigger ripening and carotenogenesis.